DESIGN OF A

HIGH PERFORMANCE SOLAR SAIL SYSTEM

by

KIM ERIC DREXLER

B.S., Massachusetts Institute of Technology
(1977)

SUBMITTED IN PARTIAL FULFILLMENT
OF THE REQUIREMENTS FOR THE
DEGREE OF

MASTER OF SCIENCE

at the

MASSACHUSETTS INSTITUTE OF TECHNOLOGY

MAY, 1979

Signature of Author..
        Department of Aeronautics and Astronautics, May 24, 1979

Certified by..
                                        Thesis Supervisor

Accepted by...
                        Chairman, Department Committee

DESIGN OF A

HIGH PERFORMANCE SOLAR SAIL SYSTEM

by

KIM ERIC DREXLER

Submitted to the Department of Aeronautics and Astronautics, on May 25, 1979 in partial fulfillment of the requirements for the Degree of Master of Science

ABSTRACT

Fabrication of thin film reflecting elements in space appears to make feasible solar sails with 20 to 80 times the thrust-to-mass ratio of previously proposed, deployable, plastic-film sails. Relevant properties of thin film materials are reviewed. A system for the production of thin film reflecting elements in space is proposed. A structural concept suited to such sails is derived, and sail mass and sail construction are considered. Finally, the dynamics and control of such sails is examined.

Name and Title of Thesis Supervisor:

Walter Mark Hollister, Sc.D.
Associate Professor of Aeronautics and Astronautics

TABLE OF CONTENTS

Introduction:

Plastic film materials chosen for use in deployable sails have masses around fifty times higher than those of thin, reflective aluminum films, on a per unit area basis. Since the acceleration of a solar sail is inversely proportional to its mass per unit area, successful exploitation of thin film reflectors would result in solar sails of markedly improved performance. The delicacy of thin film materials appears to preclude successful launch and deployment (in the large areas needed for practical sails), necessitating their fabrication in space.

Use of thin metal films as reflectors for solar sails has been suggested several times in the past (Wiley, 1951; Tsu, 1959). A method for fabricating such films in space has been proposed (Lippman, 1972), but experimental work with this method (which involved attempts at peeling the films directly from a solid substrate) failed to produce films less than 500 times thicker than films that the author has made, handled, and suggests making in space.

The chapters that follow discuss the properties of thin films, the design and manufacture of thin film elements suitable for use in sails, an efficient structural concept, sail construction, and sail dynamics. Since

this is a design study, more effort has gone into the design and redesign of the various system elements than into detailed analysis of particular point designs. Each of the major system elements has undergone some four to six major revisions in the course of this work; in each of these revisions design and analysis were carried far enough to bring out most of the major problems and system features as a guide to further work. Many problems of analysis and optimization are suggested by the present work, and considerable review and analysis will be required to determine whether major problems have gone unnoticed, and whether the preliminary analysis of the problems that have been addressed is substantially correct. Some of these matters will be dealt with further in MIT Space Systems Laboratory Report 5-79.

The concept described below is designed for high performance sails, large production rates, and low incremental production costs. In short, these designs were developed with heavy sail utilization in mind. While the results are promising enough to suggest that heavy sail utilization may eventually develop, considerably more work will be needed to determine the appropriate tradeoffs for early, small-scale production of sails for well-defined mission applications.

Chapter 1: Thin Films for Solar Sails

1.1: Criteria for choice of the reflecting material

A reflecting material for a solar sail film must reflect light well in thin layers, must not melt, evaporate, or otherwise degrade, and should be as low in mass as possible. While its strength is also of interest, this may be supplemented (at a penalty in mass) by a reinforcing film of a stronger or otherwise superior material.

For a thin film to reflect well, it must have the free conduction electrons characteristic of metals (dielectric reflecting stacks are comparatively thick). In the thickness range under consideration (15 to 100 nm), most non-metallic materials are virtually transparent, although some non-metallic conductors (e.g., carbon) have low enough transmissivity in thin film form to yield some thrust.

Absorption of light by the sail has undesirable effects beyond simple loss of thrust relative to a sail with higher reflectivity. For one, the absorbed light exerts a force directed radially from the sun. This component of thrust is often a handicap for high-performance, lightly-loaded sails on fast heliocentric trajectories. In addition,

absorbed light heats the film, raising its equilibrium temperature in proportion to the fourth root of its absorptivity.

Other physical properties are also of importance. The thermal properties of a material place limits on how closely a sail built from it may approach the sun (the Icarus syndrome). To avoid evaporation or certain mechanical instabilities, the material must have a low vapor pressure (or a good protective coating) and an adequately high melting point. Low density metals are preferred to minimize the sail's mass. A final consideration is the film's strength, toughness, and creep resistance, although these can be supplemented by reinforcement.

For a variety of reasons, this study will concentrate on aluminum as a reflecting material for the sails. It has high reflectivity, low density, a resaonable melting point, and a very low vapor pressure. Further, it has received extensive study in thin film form by various workers. The author has had enough experience with thin aluminum films to give him a measure of confidence in their ability to survive suitably delicate handling. Relevant examples from this experience will be cited fromm time to time. Still, other metals (magnesium?) could prove attractive. As will be seen in Chapter 5, however, the choice of a film material and thickness can be left open until very late in the sail development program itself with little impact on other system elements, and hence need scarcely be settled at this stage.

1.1: Thin aluminum films for solar sails

1.2.1: Optical properties

Figure 1.1 plots the reflectivity and transmissivity of aluminum films as a function of their thickness, for light with a wavelength of 600 nm. Contrary to what one would suppose from an intuition based on the concept of skin depth, reflectivity for short wavelengths falls off faster with decreasing film thickness than that for longer wavelengths, in good conductors (Barnes, 1931). Consequently, any aluminum film thick enough to reflect well in the visible wavelengths should reflect even better in the infrared, where roughly half of the sun's power output lies. Even in the visible wavelengths aluminum's reflectivity remains near its bulk value down to a thickness of 30 nm, and remains above 0.8 down to about 15 nm. (Note: at the Earth's distance from the sun, a "sail" consisting simply of a 15 nm aluminum film would accelerate at about 20 cm/s^2!)

The reflectivity of aluminum films varies with deposition conditions (Hass, 1961). Over a range of at least 303 to 473°K, reflectivity increases with decreasing substrate temperature. In the author's experience, films deposited at 250°K were quite reflective. High deposition rates, near-normal vapor incidence, and a good vacuum all favor high reflectivity. In general, poor deposition conditions reduce reflectivity for the shorter wavelengths more than for for longer wavelengths, and thicker films are more sensitive to vapor incidence angle than are thin. Since most of the sun's power output is at comparatively long wavelengths, and since the films are to be quite thin, poor deposition conditions should not greatly affect sail performance. The device described in Chapter 2, however, should provide excellent deposition conditions.
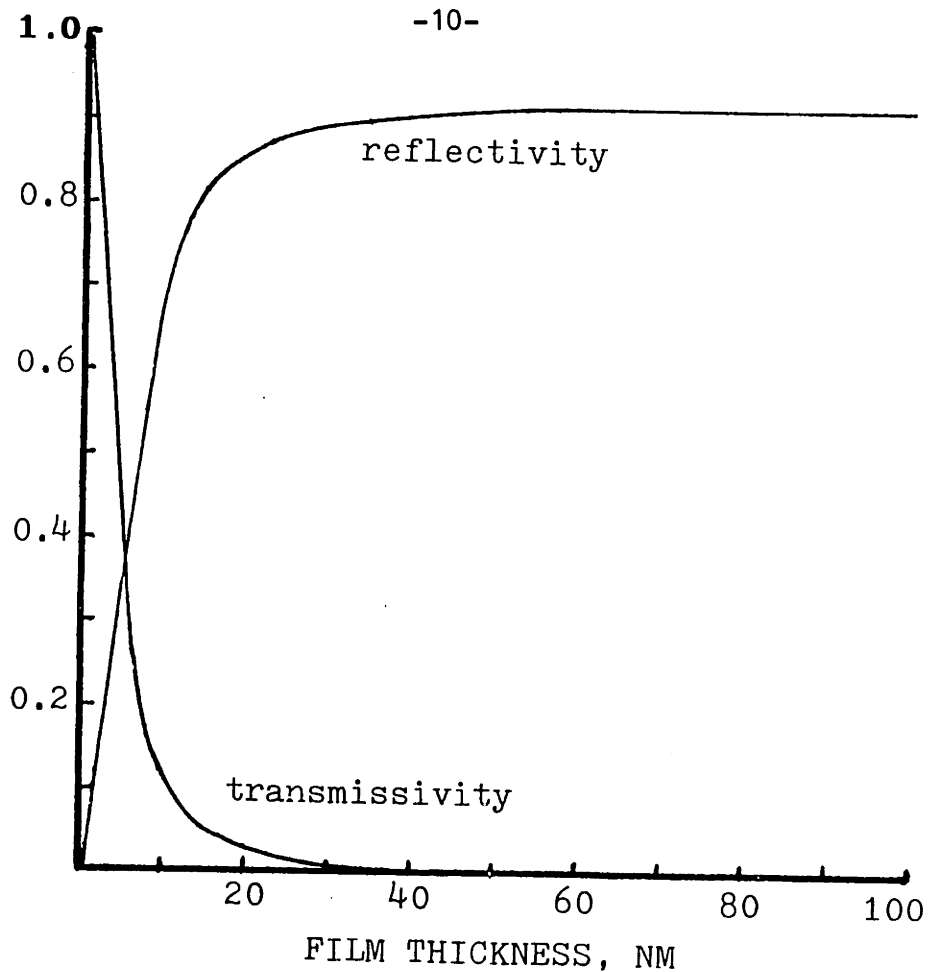
Fig. 1.1: Reflectivity and transmissivity of aluminum films as a function of their thickness.

To determine the forces on a solar sail accurately would require essentially complete knowledge of the film's optical properties. This study will simply approximate the reflectivity as 0.85 and the absorbtivity as 0.15, which are probably conservative values.

The emissivity (e) of an annealed, unbacked 98 nm aluminum film was reported as 0.05 at 425°K, and 0.06 at 725°K (Boiko, 1973). Assuming the pessimistically high value of solar absorptivity (a) given above yields an a/e of 3 to 2.5 for the film. Temperature calculations in this study will assume the still more pessimistic value of 5.2 (typical of bulk aluminum

(Hunter, 1973)) for both surfaces of the sail, despite the likelihood of the aluminum film's being backed with a reinforcing layer of higher emissivity.

1.2.2: Film temperature

Under the worst-case assumption that it is normal to the sun's illumination, the equilibrium temperature of the film is

$$\left(\frac{1}{2R^2} \frac{a}{e} \frac{P_\odot}{\sigma}\right)^{1/4} \, {}^\circ K$$

where σ is the Stefan-Boltzmann constant, R is the distance from the sun in astronomical units (AU), and $P_\odot$ is the solar constant (1353 W/m^2) at one AU. Assuming the above value for a/e, the equilibrium temperature at one AU is 499°K, rising to 705°K at one half AU. This is to be compared with the 725°K temperature that aluminum films were subjected to in the above experimental work on emissivities.

1.2.3: Agglomeration of low-melting films

Above some temperature, thin metal films fail by agglomeration. This occurs because thin films have an enormous ratio of surface to volume, permitting them to substantially reduce their surface energy by forming droplets. Above the melting point, the material rearranges swiftly, like a soap bubble bursting. At temperatures somewhat below the melting point, agglomeration into droplets occurs far more slowly, through surface

diffusion. Threshold temperatures for such processes typically scale with the melting temperature of the material, permitting one to draw analogies between different material systems.

Thin films made from silver, with a melting point of 1235° agglomerate at less than 500°K (Seraphin, 1976): the analogous temperature for aluminum is a mere 378°K. Nevertheless, aluminum films have survived 15 minute anneals at 673°K (Ferraglio, 1967), and two hour anneals at 700°K (Boiko, 1973). The latter reference presents data taken from films at 725°K, and refers in its abstract to experiments at 900°K, within 33 degrees of aluminum's melting point. The reason for this pleasing discrepancy is the presence of an oxide layer on the aluminum, which armors the surface with a rigid, refractory skin, thereby inhibiting surface diffusion and preventing changes of shape.

The conclusion that the presence of a refractory surface layer inhibits agglomeration is supported by experiments in which silver films were rendered stable to hundreds of hours of annealing at 813°K by sandwiching them between two layers of chromium oxide (Seraphin, 1976). Similar results have been reported for other materials, supporting the notion that the special properties of the film formed by the natural oxidation of aluminum are unimportant to the stabilization of the film.

1.2.4: Creep

Since the films are to be hot and mounted under tension, creep is of concern. This leads one to consider the stress state inside a simple aluminum thin film. The interior of a small droplet will be in

compression, because of its surface energy and the resulting force of surface tension. In like fashion, the interior of a thin film will be in compression (Hoffman, 1966), unless the mounting tension exceeds its surface tension. Taking the surface tension of molten aluminum, 0.84 N/m (CRC Handbook of Chemistry and Physics, 52nd edition), as a lower bound on the surface tension of solid aluminum, 56 MPa (about 8,000 psi) is a lower bound on the compressive stress in an untensioned 30 nm film.

Consider an oxide-coated film: to elongate it must not only break the oxide skin (which may be very strong), but must also create fresh, uncoated aluminum surface, requiring a force greater than surface tension to do so. To shrink, on the other hand, it must somehow crush or destroy the oxide surface, which its clearly cannot do. In fact, "shrinkage" would manifest itself as agglomeration, which was discussed above. In designs where the tensioning forces are less than surface tension, creep should be no problem, even in ordinarily creep-prone materials.

1.2.6: Mechanical properties

The strengths of a variety of thin metal films and thicker vapor deposited sheets have been measured experimentally. Metals in thin films have mechanical properties differing from those of the bulk material, because of the close proximity of all parts of the film to the surface.

Figure 1.2 summarizes data from Millillo, 1969, on the strength of aluminum films as a function of their thickness at ordinary temperatures. Note that the yield and fracture stresses increase as the film gets thinner; this behavior is typical of other metals as well. Aluminum films

showed substantial ductility, and a variable degree of plastic deformation before failure. Low, irregular values of the modulus (in the range of
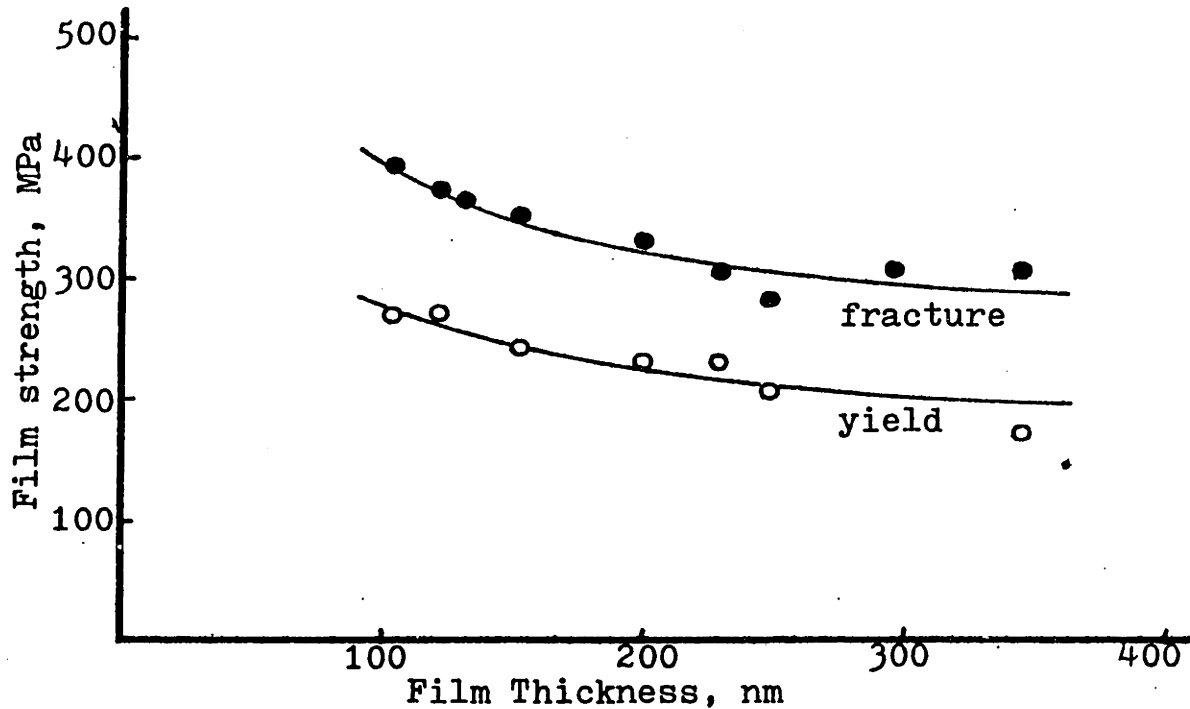
Fig. 1.2: Fracture and yield stresses in aluminum films

10,000 to 20,000 MPa) were reported for the same set of films.

Gold films less than 50 nm thick exhibit no plastic strain before fracture (Hoffman, 1966), and hence presumably lose much of their tear resistance. This loss of plasticity is believed to result from the pinning of dislocations by the surface; consequently, other metals should show the same phenomenon below some thickness. The scarcity of data in the literature on the strength of films much below 60 nm thick supports this notion. In the author's limited and qualitative experience, aluminum films seemed to become disproportionately more fragile as they became thinner, below an estimated thickness of 60 nm.

1.3: Reinforcing films

Aluminum films of the minimum thickness required for essentially full reflectivity may prove too weak to support the stresses imposed on them during fabrication and operations, or may creep under load at elevated temperatures. If so, it seems natural to strengthen them, not by adding further aluminum, but by adding a reinforcing film of a stronger, more refractory material.

1.3.1: Design considerations

A good reinforcing film should be strong, light, and easy to deposit. It need not be chemically compatible with aluminum, since a few nanometers of some other material can serve as a barrier to diffusion. A reinforcing film is apt to have such a high modulus that it will act as the sole load bearing element in the composite film. The aluminum film could help contribute tear resistance, however.

The use of a metal as a reinforcing film should reduce the amount of aluminum needed to give good reflectance. Some metals, such as nickel, may reflect well enough to be of interest by themselves.

Ceramics are among the strongest materials, and many have been prepared in thin film form. Unfortunately, there has been little interest in unbacked thin films of most ceramics, and still less interest in measuring their mechanical properties. Thin, unbacked films of various metals have drawn study for three major reasons: as thin, elemental

targets for nuclear studies, as filters transparent to energetic photons but opaque to visible light, and as micro-samples for basic research on metals. Ceramics, unfortunately, are generally not elemental, lack special optical properties in thin, unbacked layers, and are not metals. Nevertheless, the strength of certain ceramics in bulk form, the general tendency of thin films to be strong, and various information in the literature all suggest that some of these materials may make excellent reinforcing films. Many structural metals and ceramics could have been mentioned as candidate materials, but data is sparse.

1.3.2: Candidate materials

Films of pure titanium some 250 to 2,000 nm thick were found to have strengths of 460 to 620 MPa (Pickhardt, 1977), while vapor deposited foils of Ti-6Al-4V some 40,000 to 2000,000 nm thick had tensile strengths of 970 to 1,200 MPa, and met aerospace materials specifications for use in honeycomb structures. (Smith, 1970). Titanium has enough strength and temperature tolerance to make it an attractive choice as a reinforcing film. Unbacked films 52 nm thick and 0.8 cm across are reported (Rustgi, 1965).

The strength of nickel films exceeds 2,000 MPa at thicknesses of 70 nm or less, dropping to 1,500 MPa on annealing (Hoffman, 1966). Nickel's density is a disadvantage for use in sails of the highest performance, but should prove acceptable for bulk transport sails.

Silicon monoxide is a popular thin film material with many uses. On aluminum, these films have found extensive use as satellite thermal control

coatings, and have demonstrated their stability in the space environment. Unbacked aluminum thin films with SiO coatings have been made for use in space (Hunter, 1973). Mounted on fine metal meshes, unbacked SiO films as thin as 2.5 nm have found use as specimen supports in electron microscopy (Hall, 1966); such films are described as having "great strength," and are so stable at high temperatures that they may be cleaned by passing them rapidly through a blue gas flame. Since SiO is easy to evaporate, is refractory (melting point = 1970°K), has a low density (2.13 gm/cm^3), is apparently of high strength in extremely thin film form, and is of known space compatibility, it shows promise as a reinforcing film material.

Vapor deposited boron films have strengths of 620 MPa (Beecher, 1967). Since it is light and refractory, boron may prove desirable as a reinforcing material.

Carbon forms amorphous films of "exceptional strength;" those used in electron microscopy are made as thin as 4 nm (Hall, 1966). Since carbon is strong, light, refractory, and easy to deposit, it is a promising material for reinforcing films.

1.4: Design of the thin film sheets

1.4.1: Shape and size

For a wide variety of reasons, the sail will not be one big piece of film, but rather many smaller sheets mounted on a structure. Since the fabrication device will produce strips, natural choices for the shapes of the sheets include long strips, shorter rectangles or squares out from the

strips, and triangles cut from the strips. These sheets must be tensioned, and should be plane. Since a triangular sheet will be plane if tensioned at its corners, and since triangular sheets will fit well into a fully triangulated structure, they will be used as a basis for further design work here.

The width of the strip will determine the altitudes of the triangular sheets. The fabrication system described in the next chapter produces strips one meter wide, yielding equilateral triangles 1.15 meters on a side and 0.575 square meters in area.

1.4.2: Tear-resistant sheet design

Tears are a critical concern in the use of thin films for solar sails. While even sheets of extremely thin material have adequate strength to support the loads expected during fabrication and operations in the absence of stress concentrations, the inevitability of manufacturing flaws and micrometeoroid damage makes this a small comfort. While subjecting the film to only a small fraction of its fracture stress will leave small flaws stable, on large thin sheets exposed to space for prolonged periods, meteoroid damage is still apt to start tears. A means of limiting the spread of tears would be desirable, as it would allow a thinner sheet to tolerate greater damage without failure.

The most obvious method of limiting tears is to mount the film on a supporting mesh. Indeed, since thin aluminum and gold films have flown into space so mounted on several occasions, this may be considered a proven method (Hunter, 1973; Hemenway, 1975). However, differing coefficients of

thermal expansion and differing temperature between the mesh and the film are apt to make the film become slack and lose its flatness, or become taut and possibly tear. Further, the mesh adds mass to the sail, and, because it must be fabricated, transported into space, and attached to the film, adds cost as well. Still, with modest sacrifices in performance from slackness and added mass, a mesh support will apparently work. This approach has the potential advantage, moreover, of reducing the film stresses to virtually zero.

As will be seen in Chapter 3, the operational stress in even quite high performance sail films is a factor of several hundred below their fracture stress. Since the problem is not so much the stress as the propagation of tears, a natural approach to tear-stopping is to subdivide the film, converting it from a continuous sheet to a redundant network of small, load-bearing elements. In such a structure, a large manufacturing flaw or a grazing micrometeoroid impact is free to initiate a tear---but the tear will cause the failure, not of an entire sheet, but of a small piece of film, perhaps 25 square millimeters in area.

Figure 1.3 illustrates how a pattern of cuts and wrinkles can de-tension areas of film to isolate stress in smaller regions. Each wrinkled region is fabricated with enough extra material to avoid being stretched flat as the film is tensioned. Stress isolation is aided by slits extending perpendicular to the boundaries. These slits are terminated at their stress bearing ends in a way that avoids initiation of tears. As may be seen, a tear in any region will propagate into a de-tensioned region and stop there, limiting damage to a single element. Since the reserve strength factor is so high, adjacent elements should be

able to take both the redistributed and the transient loads from element
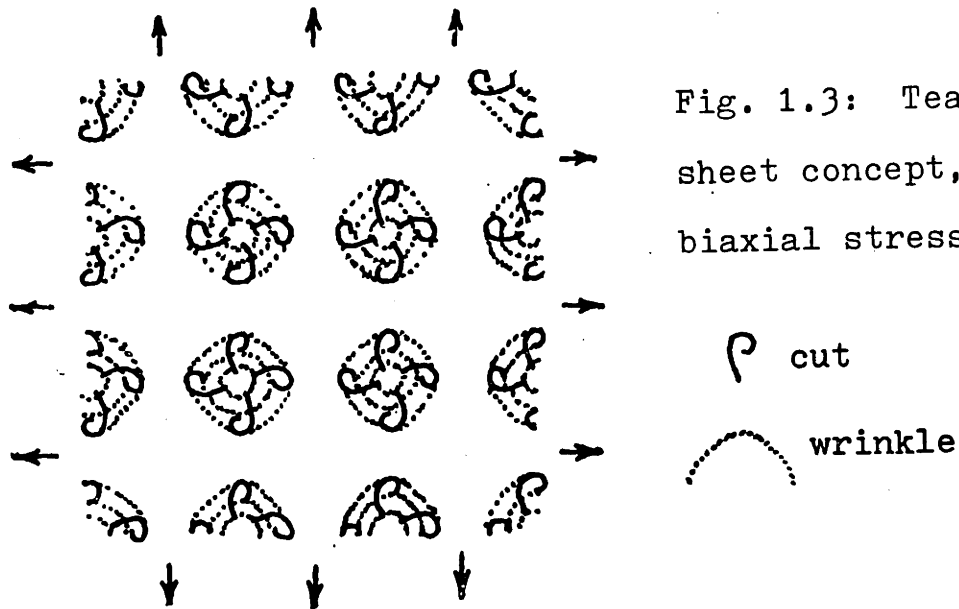
Fig. 1.3: Tear resistant sheet concept, region of biaxial stress.

$\mathcal{P}$ cut

wrinkle

failures.

Figure 1.4 shows how tears can be blocked in a region of essentially uniaxial tension, like that near the corner of a triangle. Slits, again terminated so as to avoid initiating tears, divide the film into parallel load-sharing tapes. Not shown is an alternative pattern for the main sheet, with hexagonal elements and triangular detensioned regions. Such a
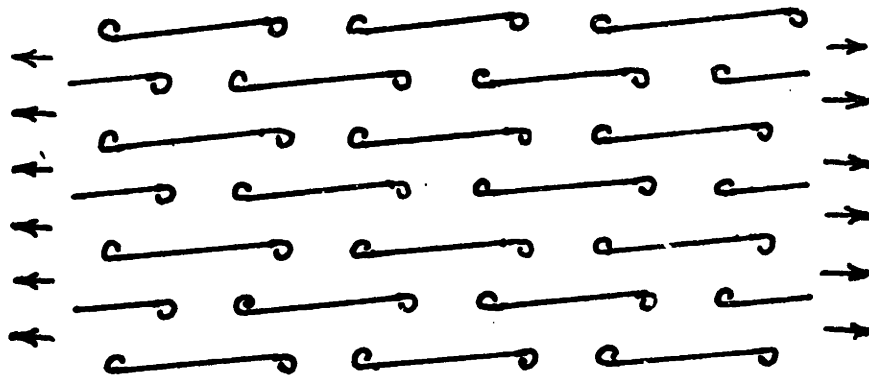
Fig. 1.4: Cuts in a region of uniaxial stress.

pattern leaves a greater portion of the sail surface flat and in tension.

While the film sheets are quite large, the small load-bearing elements are of a size similar to that of tensile test specimens made in the laboratory.

This approach to tear resistance appears superior to that of mounting the films on a metal mesh. It involves the fabrication of no additional elements, and the addition of no extra mass. By taking advantage of the natural strength of the films, it avoids slackness due to differential expansion and yields a flatter sail.

While the above describes an attractive and apparently feasible approach to the design of the film elements, a variety of questions remain regarding the detailed design. Should the film have a positive, negative, or zero curvature, in the metric sense? How should stressed and unstressed regions be distributed? Need the edges of the triangles be scalloped to avoid wrinkles, or are wrinkles acceptable, or is there another way of avoiding or controlling them? The answers to these questions will have only a small impact on final sail performance, primarily through their effect on the variance of the sail surface angle, hence a more detailed design lies beyond the scope of this study.

Chapter 2: The Film Sheet Production System

2.1: Objectives

Since vapor deposition builds up thin sheets of material atom by atom (as opposed to rolling them down from ingots), films can be made very thin. The technology of applying aluminum coatings to materials in quantity is well established (decorative papers, for example). A lower limit on unbacked film thickness may well be set by the breakage of delicate films during handling. For this reason, minimizing the stresses applied to the film is an important design objective.

Other design objectives are straightforward, if the system is to be well adapted for large-scale production. The system should have low mass, a high production rate, and minimal complexity. The author has examined many candidate approaches to meeting these objectives.

2.2: Choice of process concept

Many approaches to film fabrication may be considered. Most obviously, the film may be deposited on a solid, then peeled free.

Unfortunately, unavoidable adhesive forces prevent suitably thin films from peeling without tearing, rendering this sort of process unattractive.

The film may be deposited on a solid, then the solid may be dissolved so as to leave the film floating on the solvent, from which it may be removed. This approach works (for small areas), and is widely used in the laboratory. It has the disadvantage, however, of requiring both a solid substance and a solvent in the process, and of involving both washing and drying of the film. Simpler, related processes include deposition of the film on a solid sheet which is then melted and evaporated, or deposition of the film on a liquid surface from which it is peeled before drying.

Unfortunately, removing large areas of film from a liquid surface and drying them would probably prove difficult. In the author's experience with solid dissolution and liquid substrate processes, surface tension forces proved able to enlarge tears, once the liquid film ceased bridging them. Since the preferred film sheet design has many cuts for stress relief, and since occasional flaws and tears would be inevitable in any case, this poses a major problem. Further, removing a film sheet from a liquid surface requires a support (such as a wire mesh); removing the film from this support also poses problems. For these reasons, processes which require separation of film sheets from a liquid will not be considered further here.

This leaves processes involving deposition of a film on a solid, followed by sublimation of the solid. These have the advantage of removing the substrate molecule by molecule, a process which is inherently virtually force free.

2.3: General considerations for subliming-substrate processes

To minimize the thermal input required to heat and sublime the substrate, it should be made as thin as possible. Since the substrate strips will be fairly wide, the organic substance must be reinforced or supported by a stronger material. Invar seems a reasonable choice to minimize thermal distortion of the substrate belt during thermal cycling.

To produce reasonably smooth films with a large component of specular reflection, the substrate must be reasonably smooth. Production of the prefered film sheet design further requires that the substrate be textured, to increase the area of the film in areas to be relieved of stress. Finally, since the film itself will be impermeable, consideration must be given to the escape of subliming vapor.

One approach to substrate fabrication is to coat a metal screen with a sublimable wax, and to shape its surface by pressing it against a polished, textured roller. The holes in the mesh permit escape of the subliming vapor. This approach requires the organic substance to have forgiving mechanical properties; a stable hydrocarbon wax, p-terphenyl (Bennet, 1956), might serve (see Fig. 2.1 for its vapor pressure curve). Control of the substrate's surface finish might pose a problem, but many alternatives exist. Although the fabrication process is comparatively complex, the author has carried this approach far enough to produce a seemingly workable design.

Another approach to substrate fabrication starts with a smooth, textured metal foil, then coats it with a thin parting layer of sublimable substance. In photographic film production, liquid layers some microns
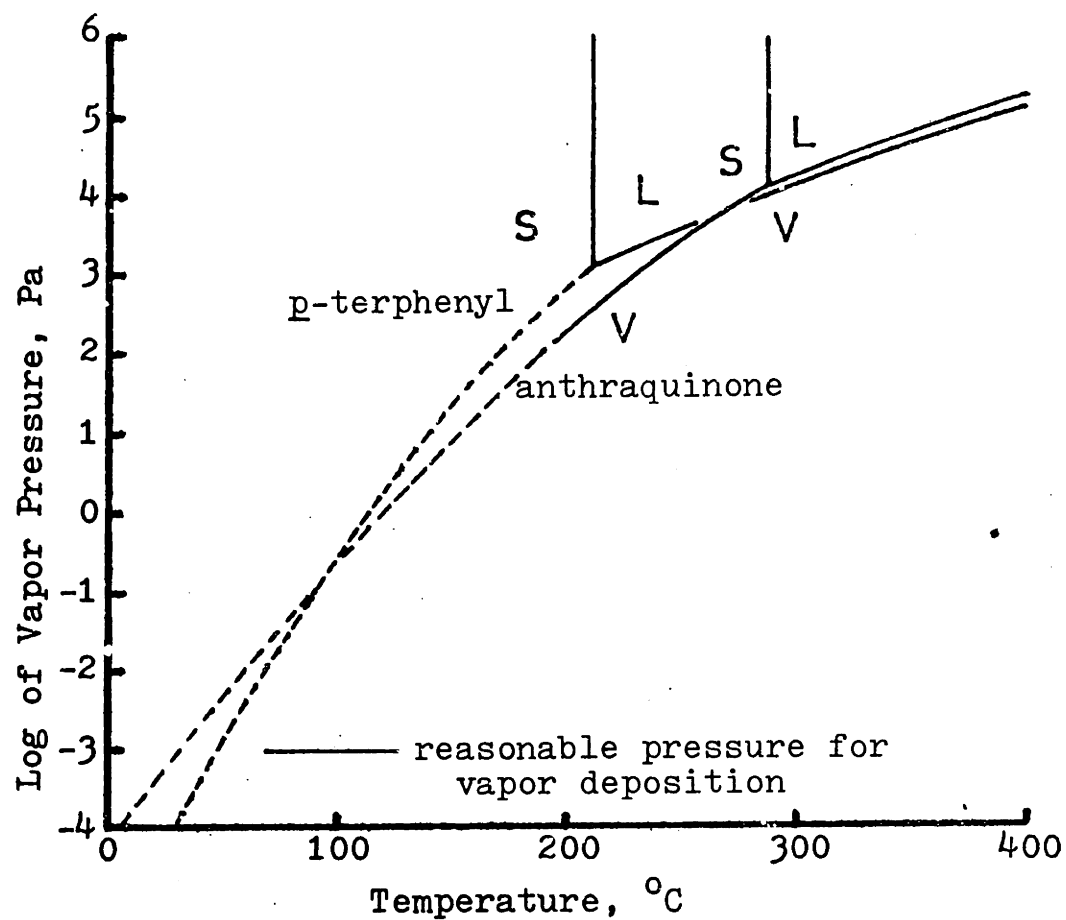
Fig. 2.1: Vapor pressure of p-terphenyl and
anthraquinone (Fritz, 1968; Kirk-Othmer, 1978).

thick are commonly laid sown. Such layers might be made to bridge pores in the foil, permitting escape of subliming vapors through the back of the substrate. Alternatively, the substance can be laid down by vapor deposition. In this case, it may be simplest for the subliming vapor to escape through holes in the film itself. This process is attractive, since vapor deposition is well understood, simple, and able to lay down very thin layers if need be. It has been selected here as a basis for further work.

2.4: Process description

Figure 2.2 illustrates the film fabrication device concept described

below.   The operations described occur in sequence to each segment of the metal foil belt as it travels clockwise around the loop.   This section presents an overview of the process; the operations will be described in more detail later.

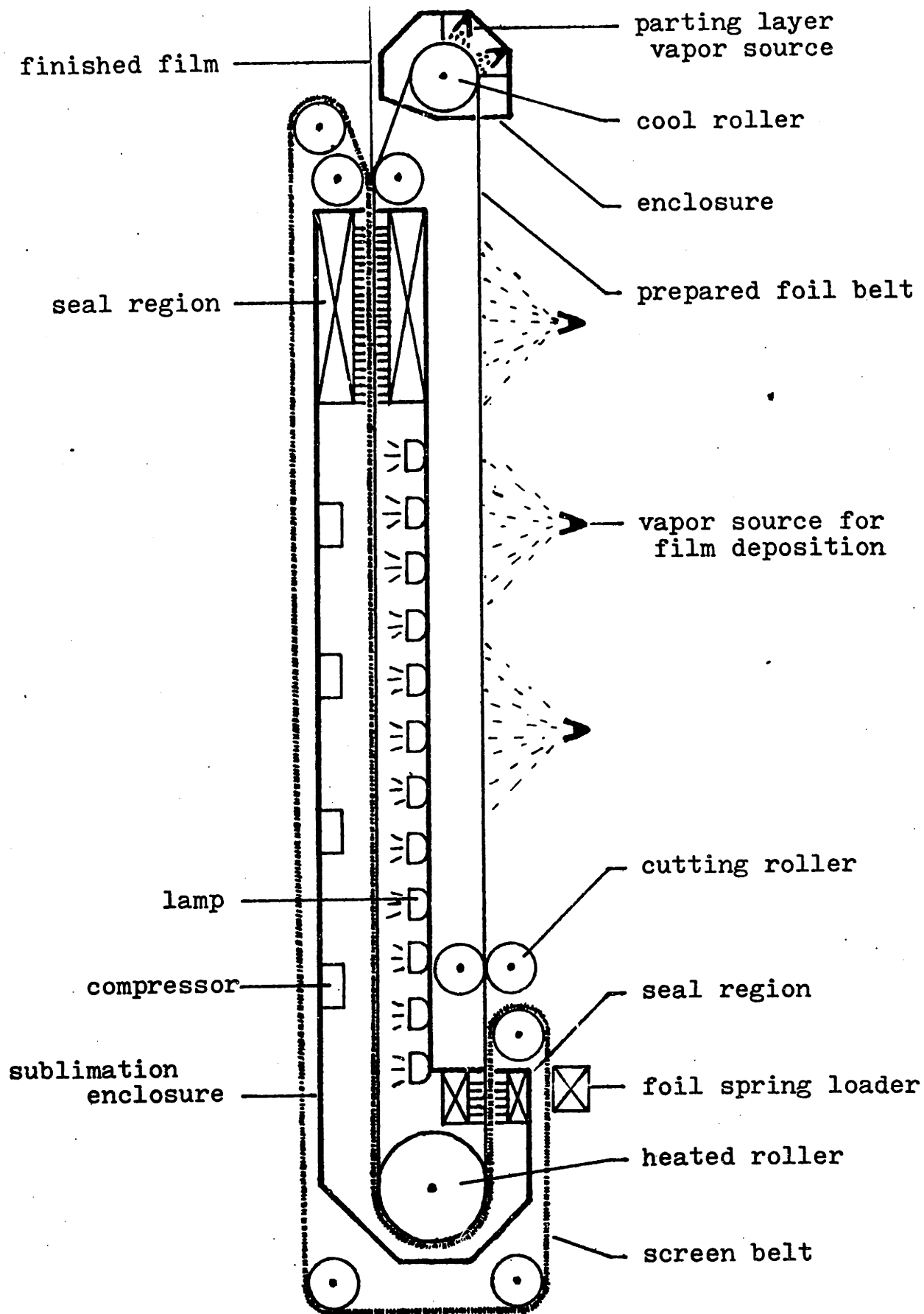The process starts as the foil belt enters the enclosure at the top of the diagram, and comes into contact with a cool roller.   This cools the belt to about 0°C, and carries it through a deposition chamber where it is coated with about a micron of a sublimable substance (such as anthraquinone, among many possibilities. See Fig. 2.1 for vapor pressure curve) emerges from this enclosure into the vacuum of space prepared for deposition of the film.

Next, it traverses a distance in vacuum, passing under a series of vapor sources.   These lay down films of material to build up the sail film. Then, it passes between two rollers which cut the film to separate it into sheets and to complete the stress relief pattern. At this point, the film sheets are ready to be mounted and freed from the substrate.

A screen belt, supported by ribs, is brought into contact with the first belt as both enter the sublimation chamber through a set of seals. The screen belt bears small metal foil spring clusters with hot melt glue on their tips.   As these heat up inside the chamber, they fuse to the corners of the film sheets, mounting them. Inside the chamber, the foil belt is brought to sublimation temperature by contact with a heated roller. It then passes in front of a series of infrared lamps which heat it further to sublime the material away. The subliming vapors escape through the cuts made earlier; the pressure differential across the film is supported by the screen and ribs of the belt facing it. Compressors and cooling coils

parting layer
vapor source

finished film

cool roller

enclosure

prepared foil belt

seal region

vapor source for
film deposition

cutting roller

lamp

compressor

seal region

foil spring loader

sublimation
enclosure

heated roller

screen belt

liquify the vapor for return to the deposition chamber.

Finally, the belts exit through a series of seals, and are decompressed gradually to let the remaining vapor escape. The film sheets, now mounted on the foil spring clusters, are carried off as the belts separate outside the chamber. The sheets are then assembled into panels (see Chapter 4); the belts re-enter the cycle.

2.5: General features of the device

2.5.1: Size

Although a considerably wider device could be accommodated in the Shuttle payload bay, the one described here is sized for strips only one meter wide. While wider strips would yield a higher performance sail (due to a reduction in the number of spring clusters and so forth per square meter of reflecting area), standard cost estimation methods suggest a higher DDT&E cost, and a higher cost for sail manufacture. The one meter strip size strikes a rough balance between these conflicting consideraions, but the choice remains somewhat arbitrary in the absence of detailed analysis.

As Fig. 2.2 shows, the device is some 12 meters long, well within the 18 meter length of the Shuttle payload bay. This length is primarily determined by the swiftness of substrate sublimation and the belt speed. The twelve meter length is based on an estimate believed to be

conservative.

2.5.2: Belt speed

Increasing the belt speed tends to increase device productivity per unit mass, but at some point leads to mechanical difficulties. A variety of industrial processes run belts, material webs, and chain drives at speeds well over two meters per second. One meter per second will be assumed in the following, yielding a device output of over 20,000,000 square meters (20 square kilometers) per year.

2.5.3: The sublimable substance

Determining the optimal properties of the sublimable substance involves a number of tradeoffs. Many materials have reasonable vapor pressure curves and other properties. For the sake of concreteness, use of anthraquinone will be assumed here. It has a triple point at about 100 Torr and 286°C, and does not decompose appreciably until much higher temperatures. It is relatively non-toxic, easing precautions in testing of the device (Kirk-Othmer, 1978).

2.5.4: Utilities

The device will have onboard electric power supplies from photovoltaics, or may be plugged into an orbiting power module. It will be equipped with a radiator and coolant loop. Attitude control is to be

provided by a larger platform of which the device would be a component.

2.6: Subsystems and operations

2.6.1: The foil belt

The foil belt is conceived of as a 25 micron thick sheet of Invar alloy. The only major disadvantage of thicker foils would be the increased power and radiator requirements arising from the greater amount of metal to be heated and cooled in each cycle. The foil may be made thicker near the edges with little penalty.

In patches corresponding to stress-relieved areas of the film, the foil must be textured. This texture consists of concentric ridges, 0.4 mm from peak to peak, with the valleys 10 microns below the peaks. This suffices to produce the stress relief bulges in the film. The surface in the textured regions, as elswhere, should be as smooth as possible.

Fabrication of such a belt might involve electron beam or laser welding to join a strip of foil into a belt, and perhaps to add thicker material at the edge. The welds could then be ground smooth. The belt could be flattened by stretching, rolling, and annealing operations, and could be textured by stamping. The smooth surface could be imparted by polishing, perhaps after deposition of a hard alloy able to take a high polish.

2.6.2: The parting layer deposition chamber

The foil belt begins its cycle when it enters the deposition chamber. Inside, it makes thermal contact with a cool roller for about a second. Good thermal contact may be ensured by surfacing the roller with a soft material, such as rubber. The roller is cooled by circulating fluid from the coolant loop down its axis. Efficient transfer of heat may be ensured by making the interior a heat pipe.

Vapor sources deposit a micron of anthraquinone on the foil belt while it is in contact with the roller (The one micron figure is fairly arbitrary, experimental work should be done here). This vapor emerges in well-directed jets from electrically heated, liquid fed evaporators, and impinges on a $0^{\circ}C$ surface. A small fraction of the vapor will miss the strip or fail to condense on impact. This remainder forms a low pressure background atmosphere in the chamber, which must be controlled.

The first step toward control is to surround the evaporators and belt with heated baffles, leaving only small clearances for the moving belt and roller. Thus, most molecules entering the atmosphere leave again by condensing on the belt, where they belong originally. Only a small fraction will escape.

By heating the chamber walls as well, buildup of condensate on these surfaces is prevented. Only the roller, which must be cool to serve its function, poses a problem in this regard, and it can be kept adequately clean with fixed, heated scrapers. The traces of vapor escaping the chamber can be kept from impinging on the rest of the device by properly placed baffles.

Since the anthraquinone layer is thin, the substrate surface will be a good replica of the foil surface. Smooth surfaces have been observed in

organic films a few microns thick.

2.6.3 Film deposition

The belt then passes under a series of vapor sources which deposit the film stack, sun-side layer first. When it emerges from the deposition chamber, the substrate's vapor pressure is around 0.0001 Pa (a reasonable pressure for vapor deposition). Further, the first layer of film to be deposited blankets the substrate, preventing further evaporation. Since the system is open to space, the vacuum is then excellent. Also, the substrate is cold, the film is thin, the deposition rate is high, and deposition is at nearly normal incidence. For these reasons, film quality should be high, limited mainly by substrate smoothness.

Vapor source design will not be dealt with in any detail here. It should be noted, however, that a wide variety of evaporators for a wide variety of materials have been used on Earth (Maissel, 1970). The major problem with evaporators on Earth is generally crucible corrosion, which may be avoided in space by levitation melting. This should permit evaporation in insulated, refractory boxes with apertures for escape of the vapors (Drexler, 1976). Such sources should be quite efficient, and should permit comparatively good control of the vapor flux distribution. The following will assume 20% efficiency of energy use in evaporation, and 20% loss of materials. These assumptions are probably conservative. It should be noted that waste heat from the evaporators will radiate directly to space, adding no burden to the cooling system.

Control of film thickness is a multi-dimensional problem. One dimension

is spatial: the more uniform the thickness distribution across the width of the strip, the more evaporators needed, introducing a design tradeoff. Also, deposition of thicker reinforcing films only where they are needed (around the corners of the film triangles, as opposed to all along the sides of the strip) is desirable for sails of the highest performance, but requires modulation of the vapor flux. The other dimension is temporal: to obtain a uniform film thickness as time passes requires either very stable vapor sources, or active monitoring and control of the deposition rate. Adequate control of film thickness (for ordinary sails at least) appears to present no special problems, with appropriate equipment and instrumentation.

Since vaporizing aluminum takes roughly 13,000 J/gm (CRC Handbook of Chemistry and Physics, 52nd edition), condensation of a 100 nm film will deposit about 3,500 J/m^2 of heat in the substrate. If the substrate is a 25 micron thick Invar foil with a heat capacity typical of iron or nickel (0.44 J/gm-$^\circ$C), its temperature will rise by 40°C. This poses no problem, since the film inhibits substrate evaporation. This calculation neglects radiative heat transfer, which should be fairly small since the aluminum film quickly becomes thick enough to reflect infrared light. If necessary, a thicker substrate could be used, yielding a lower temperature rise.

Some of the vapor will miss the substrate, as assumed above. In most vacuum systems, this poses a cleaning problem since the vapor deposits on various surfaces of the device. In this system, the substrate shadows most of the rest of the system (vapor deposition is a line-of-sight process). Vapor spillover dissipates into space. The few areas not so protected can be shielded by replaceable baffles.

As with all proposed thin film processes, this one will require experimental verification. However, the close analogy to present commercial vapor deposition processes and the considerable freedom of design suggest minimal problems with the actual deposition of the film.

2.6.4: Cutting

Once the film is deposited, its continuity must be broken to separate it into sheets and to make the cuts proposed for stress relief. Further, the pattern of breaks must be in register with the texture on the belt. Finally, the belt itself must not be damaged.

Film continuity can be broken by running the belt between two rollers, one bearing cutters which press through the film and into the organic layer. To keep the patterns in register, this roller can have a slightly variable radius, under active control. To avoid damage to the belt, the cutters should be of an elastic material considerably softer than steel, perhaps a hard plastic.

2.6.5: The screen belt

Inside the sublimation chamber, the thin film will be supported by a screen belt. This is a belt with a screen surface supported by metal ribs. It is kept at the temperature of the sublimation chamber and is brought into contact with the film at the entrance to the sublimation chamber.

A device loads foil spring clusters (see Fig. 2.3) onto clips on the screen belt as it approaches the entrance. When the two belts come into

contact, these foil springs are aligned with the corners of the film
triangles, and their tips, coated with hot melt glue, rest lightly against

foil base

handling hole
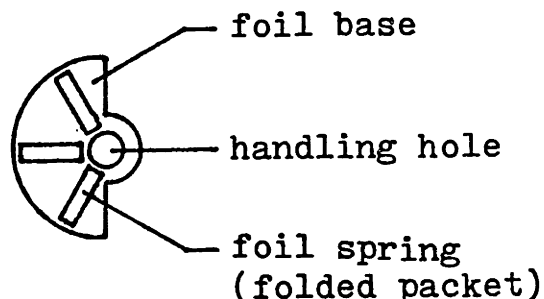
foil spring
(folded packet)

Fig. 2.3: Foil spring cluster.

the film. 2.6.5: Transfers to and from vacuum

Seals of some sort must be provided to prevent excessive escape of
vapor from the sublimation chamber. In this task, the condensabilty of
anthraquinone can be used to advantage. On the incoming side, a series of
baffles and seals can cut the leak rate from the chamber to the central
region of the seal to less than 10 gm/sec (equivalent to the leakage
through a hole about a centimeter square). The cool substrate belt can
then condense this material before it escapes through the rest of the seal
and carry it back into the chamber. The last bits of vapor can be
scavenged in cold traps and periodically recovered.

On the outgoing side, the substrate belt is hot, so this trick cannot
be used. Instead, the two belts pass through a series of small clearances
and chambers, with each chamber at a progressively lower pressure. Vapor
could be recovered from these chambers with pumps, but use of a chilled
belt to condense and carry material back into the sublimation chamber seems
a better solution. Again, cold traps can scavenge the last of the vapor.

2.6.6: Freeing the film

Conditions in the sublimation chamber are near the triple point of the sublimable substance. Under these conditions, the substance can be sublimed, compressed slightly, and recondensed to a liquid. This greatly facilitates handling.

As the belt enters the chamber, material will condense on it in a thin, dense layer until its temperature rises far enough to prevent further condensation. The belt is then brought into contact with a heated roller, which brings it to a high enough temperature to sublime the condensate and begin sublimation of the parting layer. At this point the hot melt glue fuses the foil springs to the film sheet corners.

In the sublimation process, heat may be input to the substrate by infrared lamps, as shown in Fig. 2.2, or by circulating heated vapor against the underside of the belt. Vapor escapes through the breaks in the film (special breaks may be made for this purpose, if need be), and is recovered by compression and condensation.

At this point, the integrity of the film becomes of concern, since it is being subjected to a pressure differential and is now unbacked over increasing areas. Since the anthraquinone is assumed to be one micron thick, and since it expands by a factor of 3,000 on vaporization, a 3 mm thick slab of gas must be forced through the cuts. At a velocity of one meter per second, this would take three seconds if the breaks opened as little as 0.001 of the area.

To support the film, the entire substrate belt is pressed gently against the screen belt by a small pressure differential. The mesh screen,

in turn, is supported by a track. Two issues arise: whether the film will tolerate contact with the screen, and whether the pressure differential across the film will enlarge tears. To answer such questions, the author fabricated and tested films with an estimated thickness of 40 nm. These films tolerated sliding contact with a blunt metal object. With V-shaped tears about one millimeter in size and sparse (about 0.5 cm spacing) supports, they tolerated exposure to screams of air at normal incidence with speeds in excess of one meter per second. The tears did not enlarge.

For the sake of conservatism, the sublimation chamber is designed to be much longer than three meters, and the seals at the exit point will lower the vapor's pressure quite gradually. These measures make the forces exerted on the film in the sublimation chamber far less than those successfully withstood in the experiment just described. For this reason, no difficulties seem likely in freeing films of the thickness considered.

After exit from the chamber, the foil spring clusters, now carrying the film sheets, are transferred to a conveyor and taken away to the panel assembly device. A concept for such a device is presented in Chapter 4.

2.7: Preliminary power and mass estimates

A crude estimate of the system's mass is desirable to permit a preliminary estimate of costs. Power consumption may be used to estimate power system mass. Heating the belt from 0°C to 290°C and subliming the anthraquinone takes about 26 kW. If the exit seal system must recover 10 gm/s and sublime it again, this adds about 5 kW. At the assumed 20% efficiency, deposition of a (thick) 100 nm of aluminum takes 1 kW. Another

10 kW will be allowed for heat losses and miscellaneous uses (motors, compressors, substrate deposition, etc.) Total power consumption is thus about 62 kW for a one square meter per second system. At 15 kg/kW, this amounts to 930 kg of power system.

A crude estimate of the structural mass may be made by assuming use of aluminum honeycomb with an areal mass density of 7 kg/m^2 (this should give a compressive strength of at least 300,000 N/m). A generous estimate of the mass of structure needed is that of a 1.5 m diameter tube of this material 12 meters long, plus about 20 square meters of structure of equivalent areal density in the rollers. This comes to about 540 kg. About 41 kW of waste heat must be radiated. Assuming a 300°K radiator temperature and 10 kg/m^2 of radiating area adds 1,000 kg. Allowing 530 kg for multiply redundant motors, evaporators, compressors, and so forth brings the estimated total mass to 3,000 kg.

Chapter 3: Solar Sail Structures

3.1: Tensioning Concepts

A solar sail structure must hold a large area of reflecting material in tension, must transfer normal forces from this area to a payload, and must be able to hold the reflecting material at various angles to the sun, and to change this orientation on command. In addition, it should be of low mass, easy to construct, and capable of surviving long exposure to space. Many solutions to this problem have been proposed.

Conceptually, the simplest means for tensioning the sail is a structure more or less like a kite, with stay-stiffened compression members as the sticks. This approach was explored in studies sponsored by JPL, in connection with the design of a plastic-film sail system (JPL, 1976). While the mass of the compression members in this design was a small fraction of the sail mass, it was still on the order of a gram per square meter. Since thin film technology seems to permit reflectors of some 0.04 to 0.27 gm/m^2, designs incorporating such compression members would realize only a fraction of the thin film sail's potential performance.

If a sail lacks major compression members, some other means must be

used to oppose the tension in the plane of the reflecting material. (This tension must exist to prevent the surface from ballooning out under light pressure; parachute-style sails have been shown to be unstable (Villers, 1960)) Candidate forces include electrostatic, magnetic, and centrifugal.

An electrostatically tensioned sail must have a large charge to cause adequate self-repulsion between different parts of the sail. Since space is filled with a conductive plasma, however, the charge would tend to be neutralized swiftly. JPL examined and rejected this option (JPL, 1976).

A ring of current carried by a superconductor would repel itself, and could be used to magnetically tension a circular sail. To adequately tension a one kilometer sail would require on the order of 10,000 amperes of current. If the system were allowed to add a mass of 0.1 gm/m^2 to the sail, the conductor, insulation, and refrigeration system would have to meet a mass budget of only 25 gm/m, a low value. Still, because of economies of scale, magnetic tensioning could conceivably prove desirable for very large sails.

Centrifugal force is straightforward, and can clearly tension a rotating sheet of material. It has been chosen for the design presented here. The following sections will derive an efficient structural concept based on centrifugal tensioning, and will briefly examine a specific structural design.

3.2: Derivation of an efficient structural concept

The farther a piece of sail material is from the axis of rotation, the longer the tension member required to support it against centrifugal force.

Hence there is an incentive to make spinning sails approximate disks.

The preferred design in the recent JPL-sponsored study was the Heliogyro: a centrifugally tensioned, centrifugally stiffened structure with reflectors deployed in long, narrow blades (Friedman, 1978). While such blades are structurally inefficient, the study's groundrules led to a requirement for the use of plastic film sail materials, the mass of which rendered structural efficiency a secondary consideration. Further, since the sail was to be deployable, the ease of deploying the blades from rolls together with a clever attitude control scheme involving blade pitch made this option attractive. At an earlier stage of this study (JPL, 1976), a rotating disk-shaped sail was considered and rejected, because of deficiencies in attitude control and other problems not applicable to the design considered here. It should be noted that the present design differs from the Heliogyro in being tensioned but not stiffened by centrifugal force.

The shape of a tension structure under load typically depends on the ratio of various forces in the system, in this case, those arising from light pressure and from rotation. For this reason, the ratio of the light pressure force per unit area to the centrifugal force per unit area is a parameter of interest. Call it "E."

In a spinning, disk-shaped membrane, the radial component of tension must fall to zero at the edge, by continuity. In typical designs, membrane tension will be at a maximum towards the center if the sail. The radial force per unit area, assuming constant mass per unit area, varies linearly with radius, falling to zero at the center. The force of light pressure remains constant, resulting in a distribution of force across the sail like
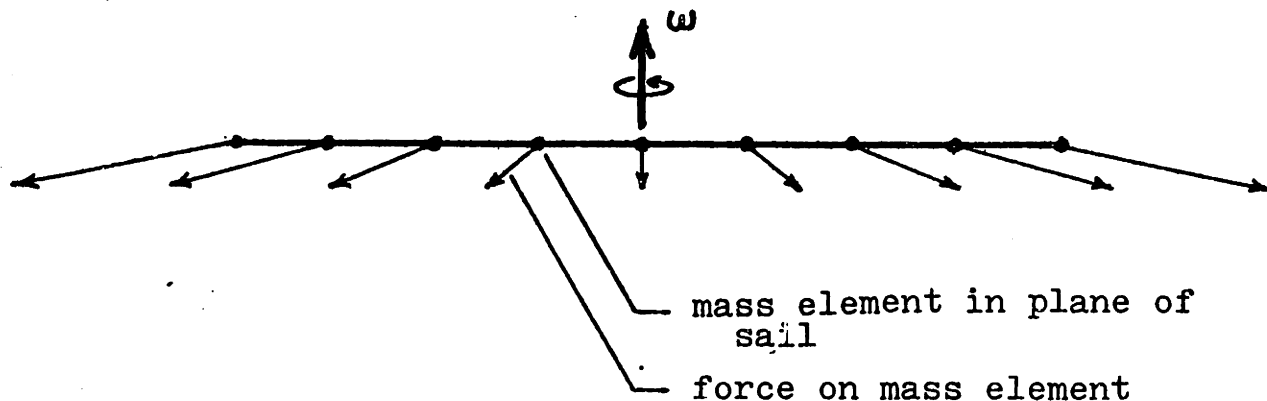
Fig. 3.1: Combined centrifugal and light pressure forces.

that shown in figure 3.1.

Figure 3.2 presents a series of sketches of idealized solar sail designs, leading from a primitive concept to a simplified version of the concept presented in more detail below. All of them represent cross sections along the axis of the sail, with the sail sheet, payload, and connecting tension menbers shown. To aid the reader's intuition, the drawings are oriented so that the force of light pressure is downwards; it may be modeled by a uniform gravitational force on the sheet. The inertia of the payload may then be modeled as a fixed attachement point from which the sail is "hung." All tension members are assumed to have negligable mass, and the shape of the sail is then sketched as it would be under the effect of "gravity" and centrifugal force.

Figure 3.2 (A) illustrates the simplest case, in which the centrifugal force is very great compared to "gravity," making the sail a taut, flat disk, "supported" at its center by the payload. Figure 3.2 (B) illustrates the deformation of the sail for a small value of E; the center of the sail is "pulled up" into a conical mound, and the edge sags at an angle of

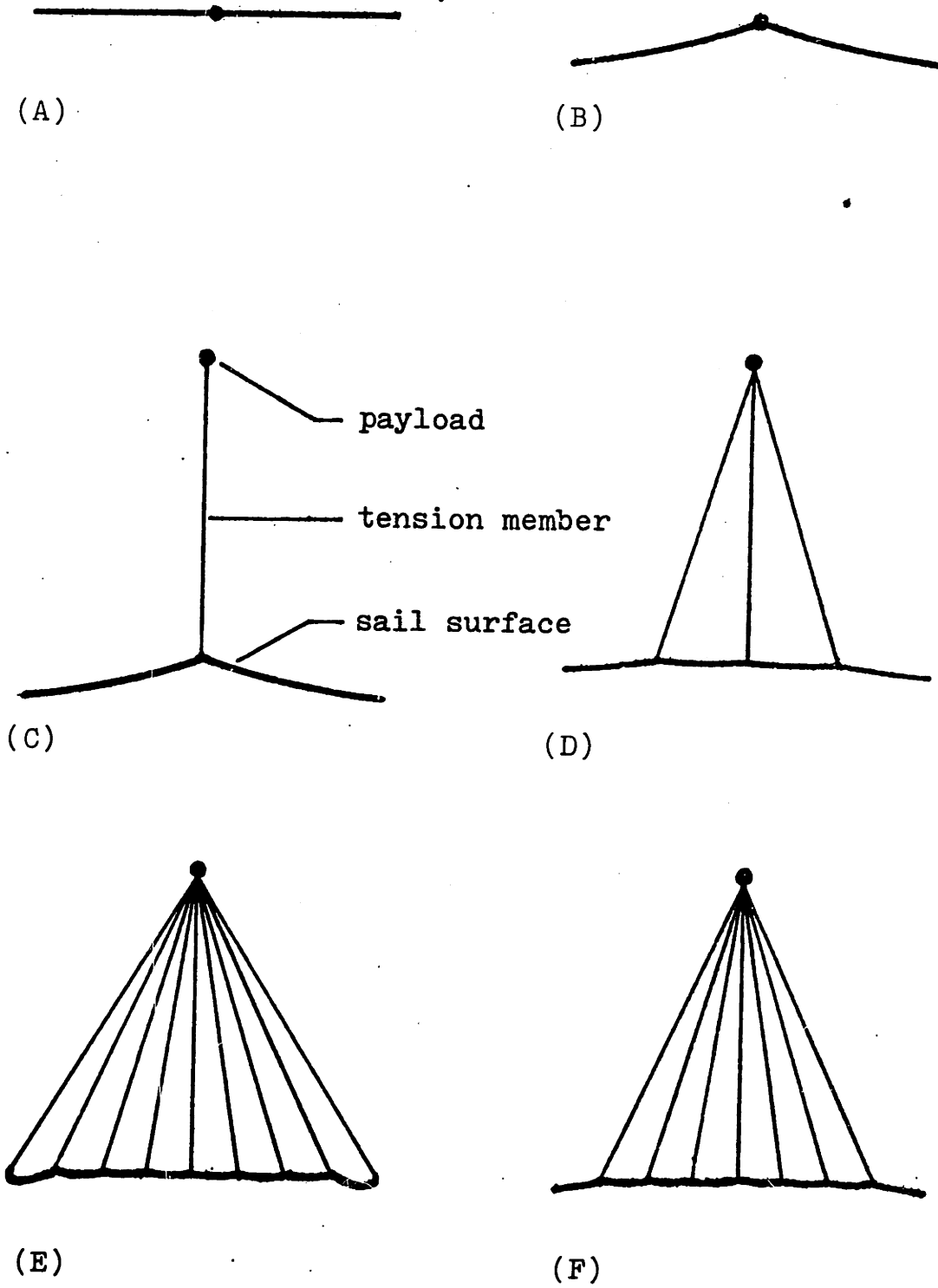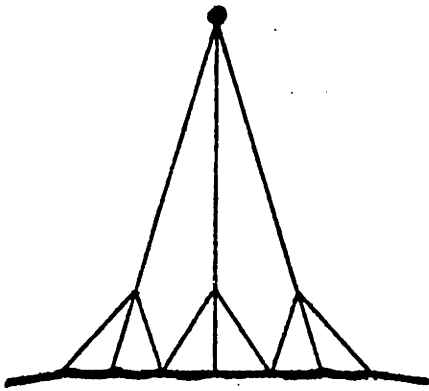Fig. 3.2: A series of solar sail designs, in cross section.

(A)

(B)
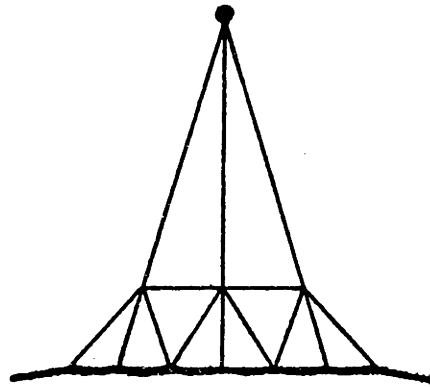
(C)

payload

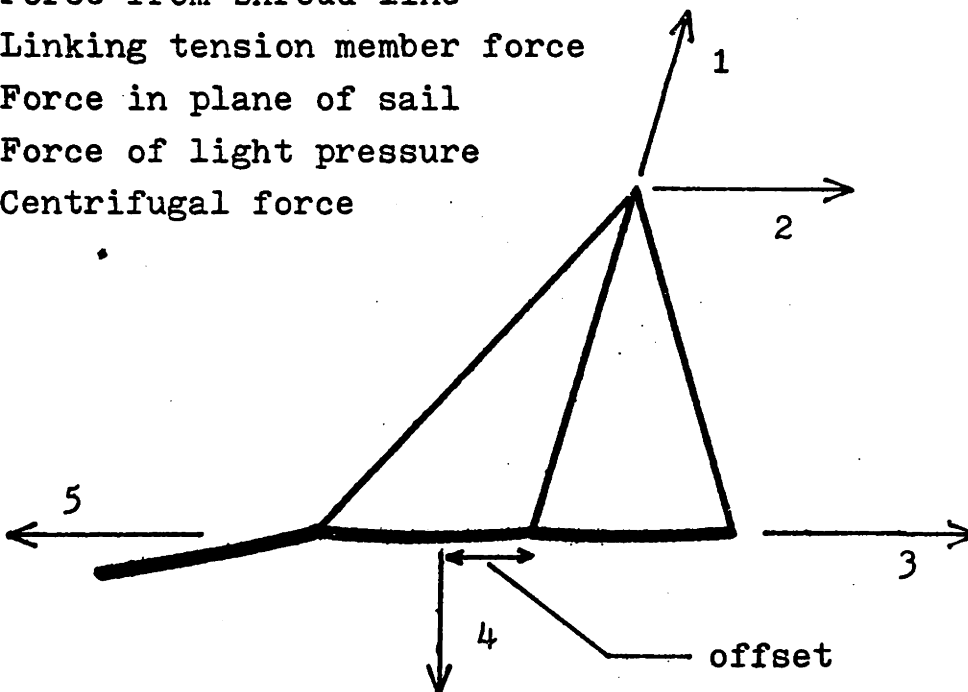tension member

sail surface

(D)

(E)

(F)

Fig. 3.2, continued.

(G)

(H)

Fig. 3.3: Forces on a section of the sail near
the edge.

1 Force from shroud line
2 Linking tension member force
3 Force in plane of sail
4 Force of light pressure
5 Centrifugal force

offset

approximately E radians. Figure 3.2 (C) illustrates that the payload may be moved in front of the sail and connected to it by a tension member with the same result.

These sail designs are not very flat (for reasonable values of E) and have stong stress concentrations at their centers. This may be alleviated, as in (D), by adding tension members to support the sail sheet at more points. Figure 3.2 (E) shows this process continued, yielding a still flatter sail for a given value of the parameter E. As may be seen in the sketch, the sail sheet sags more at the edge, where the sheet's tension is low, than near the center, where it is high. Figure 3.2 (F) shows how this excessive bagging at the edge of the sail may be eliminated by leaving the edges as free-hanging flaps. Note that the edge flap angle remains approximately E radians, regardless of inner structure.

The sail shown in (F) suffers from an excess of long, nearly parallel tension members, each carrying only a small load. Figure 3.2 (G) shows how these tension members may be bundled together in front of the sail into a lesser number of more highly stressed members. Figure 3.2 (H) then shows how the nodes created by the bundling process may be linked to make a more rigid structure.

Figure 3.3 illustrates the forces on a section of the sail sheet and the associated tension members. So long as the indicated offset between the center of light pressure on the section and the projection of the force exerted on the section by the tension member from the payload exists and is

in the direction shown, the tension members linking the bundling nodes will be in tension.

Call the members from the payload to the bundling-nodes "shroud lines," and the rest of the structure in front of the sail sheet "rigging." Since the rigging is triangulated, and since all members remain in tension, the rigging may be considered as a rigid truss. The rigging and sail sheet may then be treated as a rigid body subjected to forces by light pressure and the shroud lines. This greatly simplifies treatment of the sail's control dynamics.

This completes the derivation of a concept for a structure that will hold a large area of reflecting material in tension, and transfer normal forces from this area to a payload. As a disk-shaped, centrifugally tensioned design, it is structurally efficient and will be shown to have little mass. It remains to be shown that sails built on this concept can hold various orientations to the sun and change them on command. Before addressing this, however, a closer look at the structure itself seems in order.

3.3: The sail sheet structure

The design presented here uses a grid of tension members to carry the main structural loads (primarily those of centrifugal force) in the sail sheet. This approach maintains the integrity of the sail independent of the presence of intact panels, concentrates loads enough to justify substantial tension members, and provides firm points of attachment for the

rigging.

Figure 3.4 illustrates a hexagonal sail built around a triangular grid. This kind of design has several attractive features. Its triangulation ensures shear resistance in the plane of the structure, and minimizes the motion of nodes adjacent to failed tension members (load is redistributed well, with comparatively little distortion). Finally, the triangular apertures in the grid fit triangular panels; if these are tensioned only at their corners, they will automatically be free of imposed out-of-plane distortions. While none of these features is compelling, together they make the triangulated hexagon a reasonable point of departure for a sail design.

Its primary shortcoming lies in the high perimeter to area ratio of the triangle. Since trangulation in the rigging may provide adequate resistance to distortion, other shapes (squares?) should be considered for the grid apertures and panels.

3.3.1: Structural loads

While a detailed analysis of the sail structure lies beyond the scope of this thesis, enough analysis to indicate the general behavior of the sail and the approximate magnitude of the loads is called for to establish sail feasibility and performance. Since even a very crude analysis suggests that the structural mass fraction will by very low if the members are highly stressed, a large safety factor will be applied at the end for the sake of conservatism.

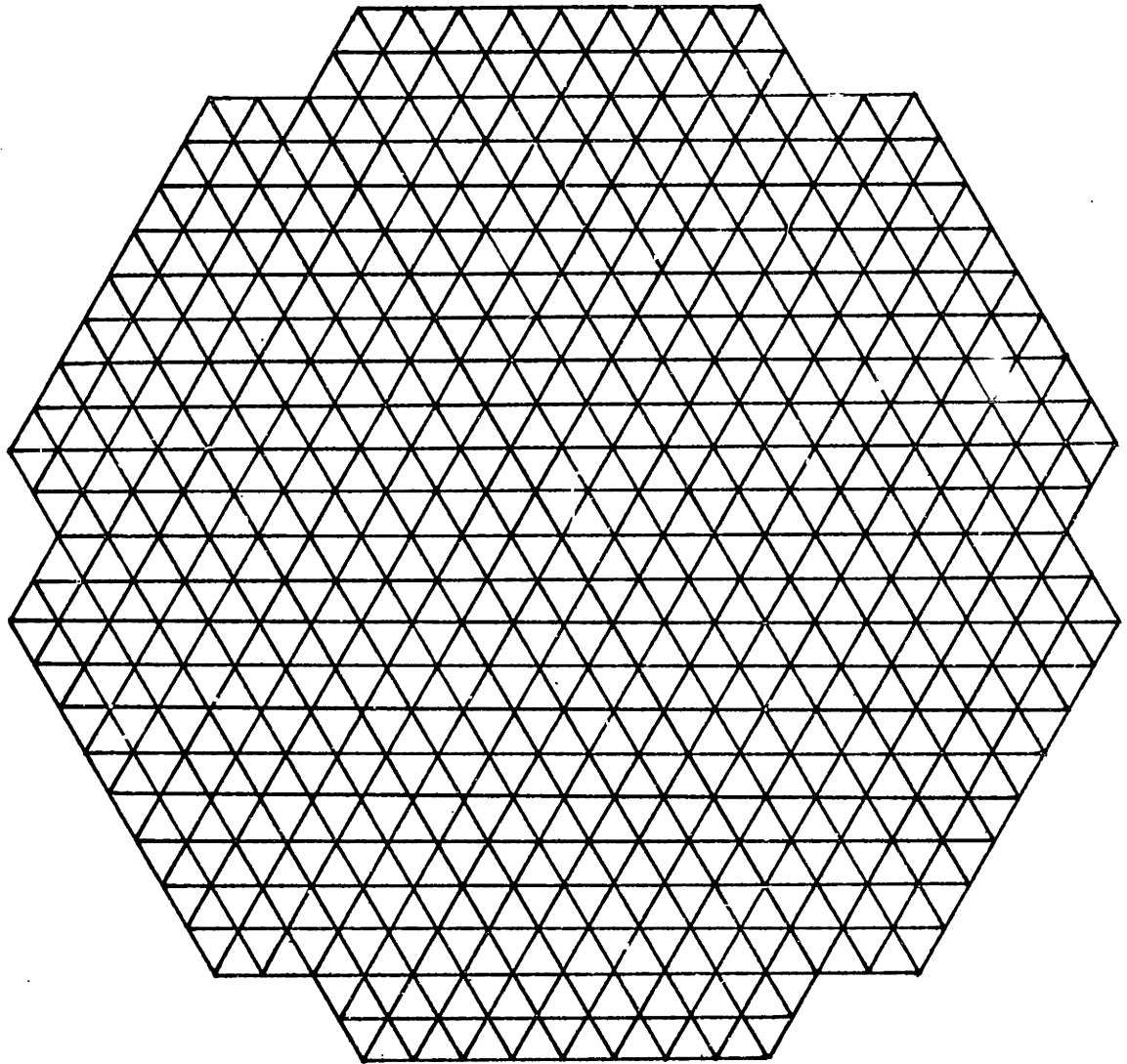Idealizing the sail sheet as a rotating, uniform disk-shaped membrane

Fig. 3.4: Structural grid for a sail 2.4 km across.

it becomes clear that the stress in the sail can vary from purely radial to purely circumferential and still support the centrifugal loads. Since the grid is statically indeterminate, control of the stiffness of the tension members can vary the distribution of stress in the sail sheet within wide limits. In practice, this could be accomplished by incorporating springs with properly chosen stiffnesses into the nodes of the structure. In

particular, the stress distribution may be made isotropic. This choice of stress distribution is in no way essential, but is only chosen for analytic convenience.

For a radial force of C (N/m^2) at the rim of a sail of radius R (m), the membrane stress S (N/m) is $(1-r/R)CR/2$, where r is the distance from the axis. This leads to an average S of $CR/4$ (N/m).

For tension members with a working stress of s (MPa), and a density of d (gm/cm^3), the mass per unit area of the sail sheet structure is $2dS/s$ (gm/m^2). The factor of two arises from the necessity of carrying stress in two dimensions, and may be verified explicitly for triangular grids.

How does this idealized result relate to a real sail? Keeping the approximation of uniform mass per unit area across the disk, the distribution of the tension forces chosen has no impact whatsoever on the average tension in the sheet: The same result may be obtained even for the extremes of purely radial or circumferential tension. Substituting a hexagon for a disk will have little impact on the structural mass. Minimum gauge considerations will increase structural mass towards the edge of the sail, but only moderately. In short, the above relation seems a good approximation to the sail's structural mass so long as the structure remains a small fraction of the mass of the sail sheet, and so long as the sail is not primarily minimum gauge limited. It will be shown below that these conditions hold for sails in a reasonable size range.

3.3.2: Sail panel design

In accordance with the ideas of the previous sections, the sail panels will be triangles composed of triangular sheets of foil, tensioned by forces at their corners. Figure 3.5 illustrates such a design. The triangular sheets are linked at their corners to form the reflecting area of the panel (the springs ensure reasonably smooth load distributiion in the face of distortion). This area is tensioned by ties connected to catenary members which are in turn connected through springs at the corners of the panel to the sail's structural grid.

Figure 3.6 shows a simplified geometric model of the panel, with the catenary members approximated as circular arcs tangent to the reflecting area and ending at the nodes of the structural grid. This model yields the ratio of the panel's area to that of the grid aperture as a function of the geometric parameter A:

The parameter A also yields an expression for the membrane stress in the panel area as a function of the tension on the corner of the panel. Taking W as the altitude of the triangualar aperture in the grid, and T as the force on a single corner, the panel membrane stress equals: For a given corner tension and grid aperture, increasing A yields an increasing membrane stress in a decreasing reflecting area.

For the sake of concreteness, A will be taken as 10° in the balance of this analysis. This yields an area ratio of 0.72, and a membrane stress of 0.224 T/W. If the panel area is composed of one meter altitude film triangles separated by one centimeter gaps, the ratio of the actual reflecting area to the total sail area (the fill factor) is 0.7.
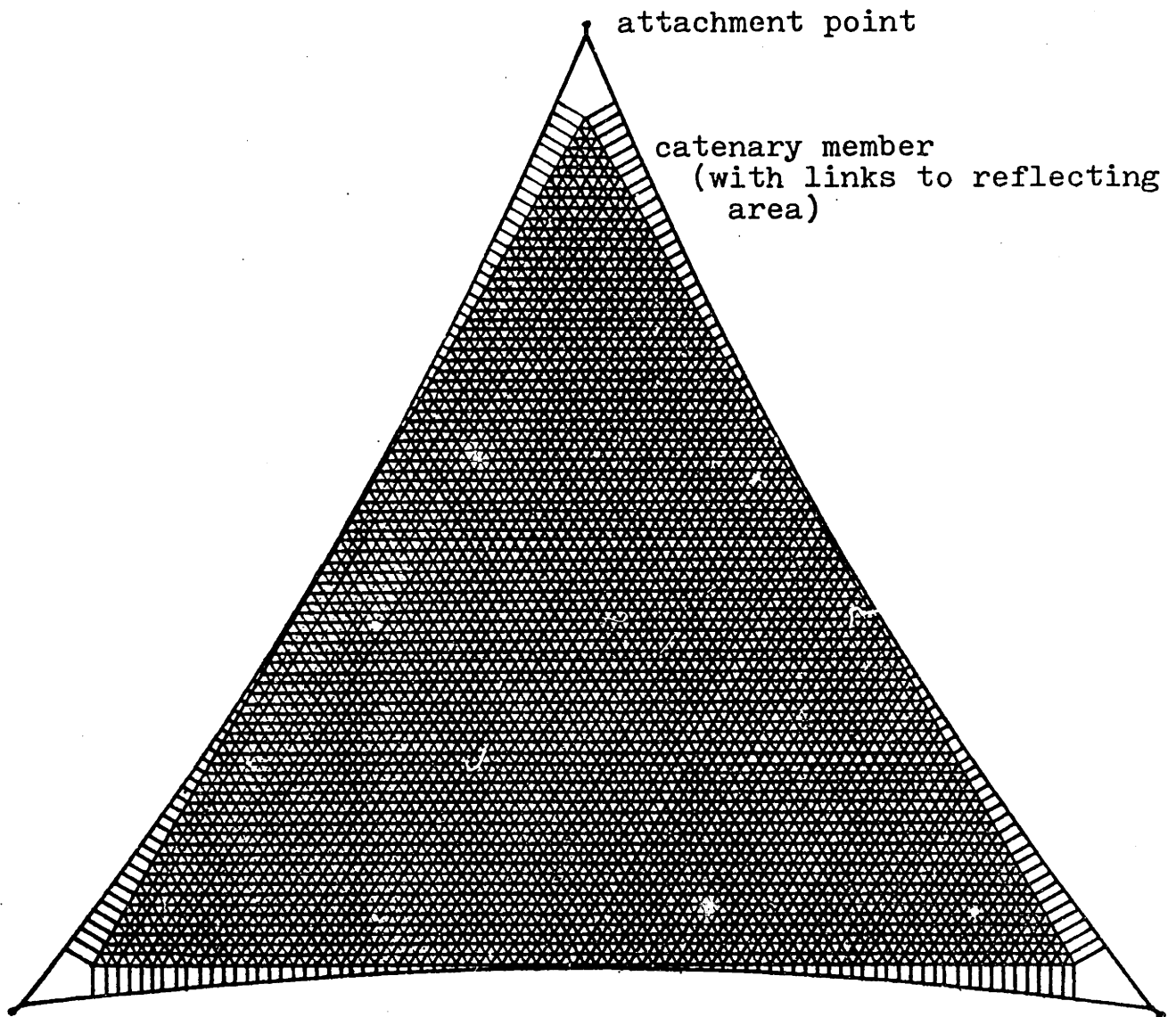
Fig. 3.5: Triangular reflecting panel with catenary
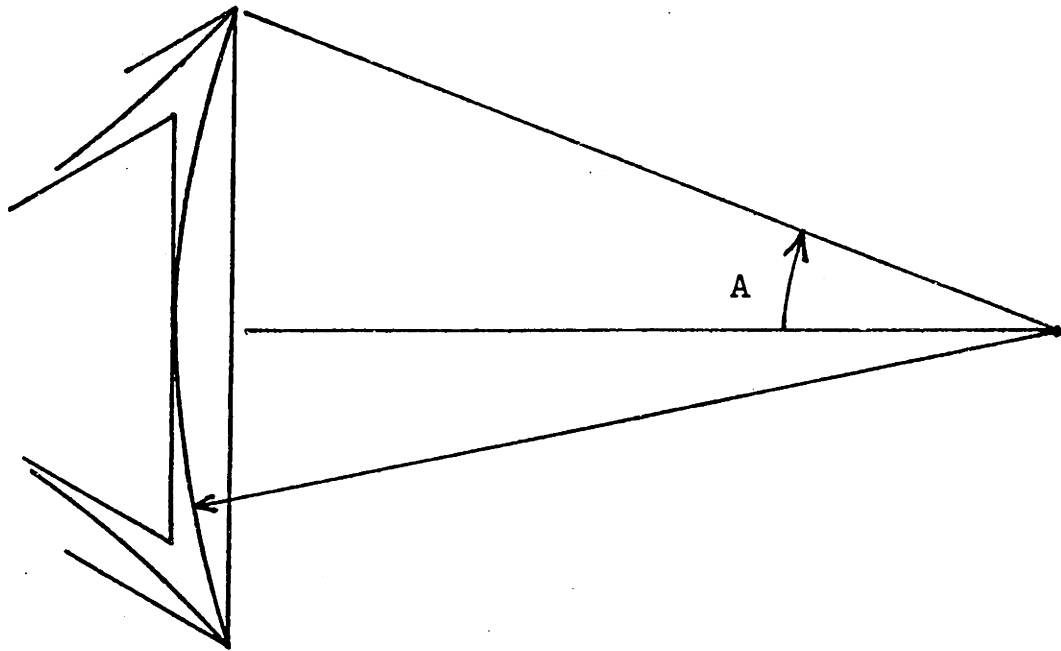tensioning members.

Fig. 3.6: Geometric model of panel, approximating
catenary members as circular arcs.

3.3.3 Tensioning panels at the edge of the sail

At the edge of the sail, continuity requires that the radial component
of the membrane stress fall to zero, in the absence of ballast at the rim.
As shown in section 3.2, maintenance of a reasonably flat surface near the
edge requires a free-hanging flap to give a finite membrane stress at the
first support point. Figure 3.3 illustrated, in one dimension, the sort of
deformations to be expected under combined light pressure and centrifugal
forces.

The triangular panels will deform under light pressure to an extent determined by their membrane stress. Solving for the exact deformation would be complex, since the catenary members deform as well. For preliminary design purposes, the panel deformation is of importance for two reasons: the degree of stretch it causes affects the design of the springs linking the film triangles, and the changes in surface angle it causes affect the sail's performance. Since these effects are not of crucial importance to the sail's design or performance, and since they depend little on the exact shape of the deformed panel, rough estimates will suffice.

The panel may be roughly modeled as a uniformly stressed membrane stretched over a circular aperture with a radius equal to one third of the length of the reflecting area's side (see Fig. 3.7). As may be seen, this yields a free span comparable to that of the middle region of the triangle. Taking the solar pressure as P (Pa), the membrane stress in the panel as S (N/m), the radius of the circular membrane as R, and the angle at which the panel sags at its rim as Q, S equals $RP/(2\sin(Q))$. The fractional deformation is roughly $1-\sin(Q)/Q$.

Taking W=100 m, and A=10°, R equals 32.7 m. Taking as a standard loading condition sunlight at normal incidence at 0.5 AU, P=3.32×10^{-5} Pa. For this force to be fully effective in producing panel deformation, the sail must further be assumed to be attached to a massive payload. Picking Q=10° for a panel near the edge of the sail, S=3.1×10^{-3} N/m, and the characteristic stretch of the membrane equals 5×10^{-3}. This deformation corresponds to a change of only 1.7 mm in the one centimeter spacing of the film triangles. This membrane stress, by the previous calculations,
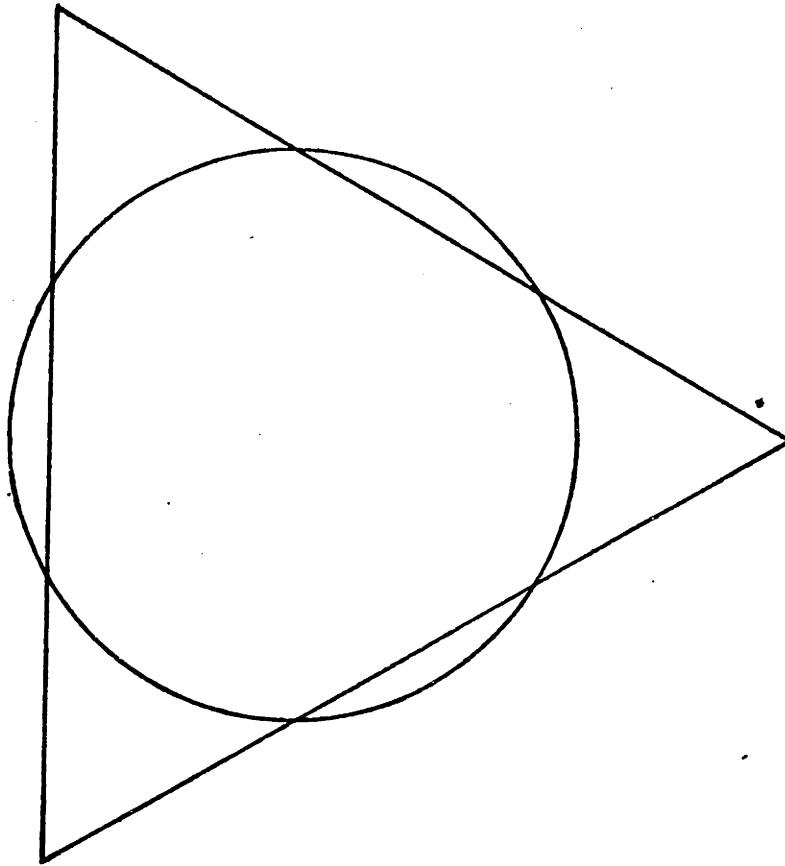
Fig. 3.7: Circle used to approximate triangle.

corresponds to a panel corner tension of 1.4 N.

Panels in the free-hanging flaps are not subject to these deformations, since the entire (local) plane of the grid is free to deflect under light pressure. In the supported area of the sail, however, the above considerations help determine the tension needed in the sheet.

Assuming that the panels take all the load in the sail sheet towards the edge of the supported area (by proper choice of spring constants at the nodes), the free-hanging flap must exert an average force of 0.012 N/m on the sheet to tension the panels as assumed above. This implies that (width

of the edge flap)x(average solar pressure)/E is greater than 0.012 N/m. Taking the flap width as 200 m (two rows of panels), E must be 0.2 or less. This makes the centrifugal force per unit area at the rim of the sail five times that of light pressure, and allows the flap to sag by about 12°.

3.4: The rigging

As Fig. 3.2 (E) indicates, the increasing membrane stress towards the center of the sail sheet decreases the sag between the points of support provided by the rigging. This immediately suggests that the center needs fewer supports for a given area. Figure 3.8 shows a cross section through a small sail rigged to take advantage of this while maintaining tolerances on the sag angles. For larger sails the benefits are still greater, and additional levels of bundling may prove desirable near the edge. Figure 3.9 shows a portion of a sail with similar rigging but with shorter shroud lines and small ballast masses to counteract the shroud's tendency to draw the rigging towards the center. These differences are associated with differing control modes, to be discussed in Chapter 5.

In either case, the rigging occupies a volume resembling a truncated pyramid. The sides of the pyramid must be concave (as shown) to maintain tension in the rigging's cross-members. The criterion given above for rigging tension ensures this.

Rigging members not perpendicular to the sail sheet will modify the tension in the sail sheet. This is of little importance save near the edge of the sail, where the angle of intersection must be considerably greater than the flap sag angle to avoid taking too much tension from the sheet.
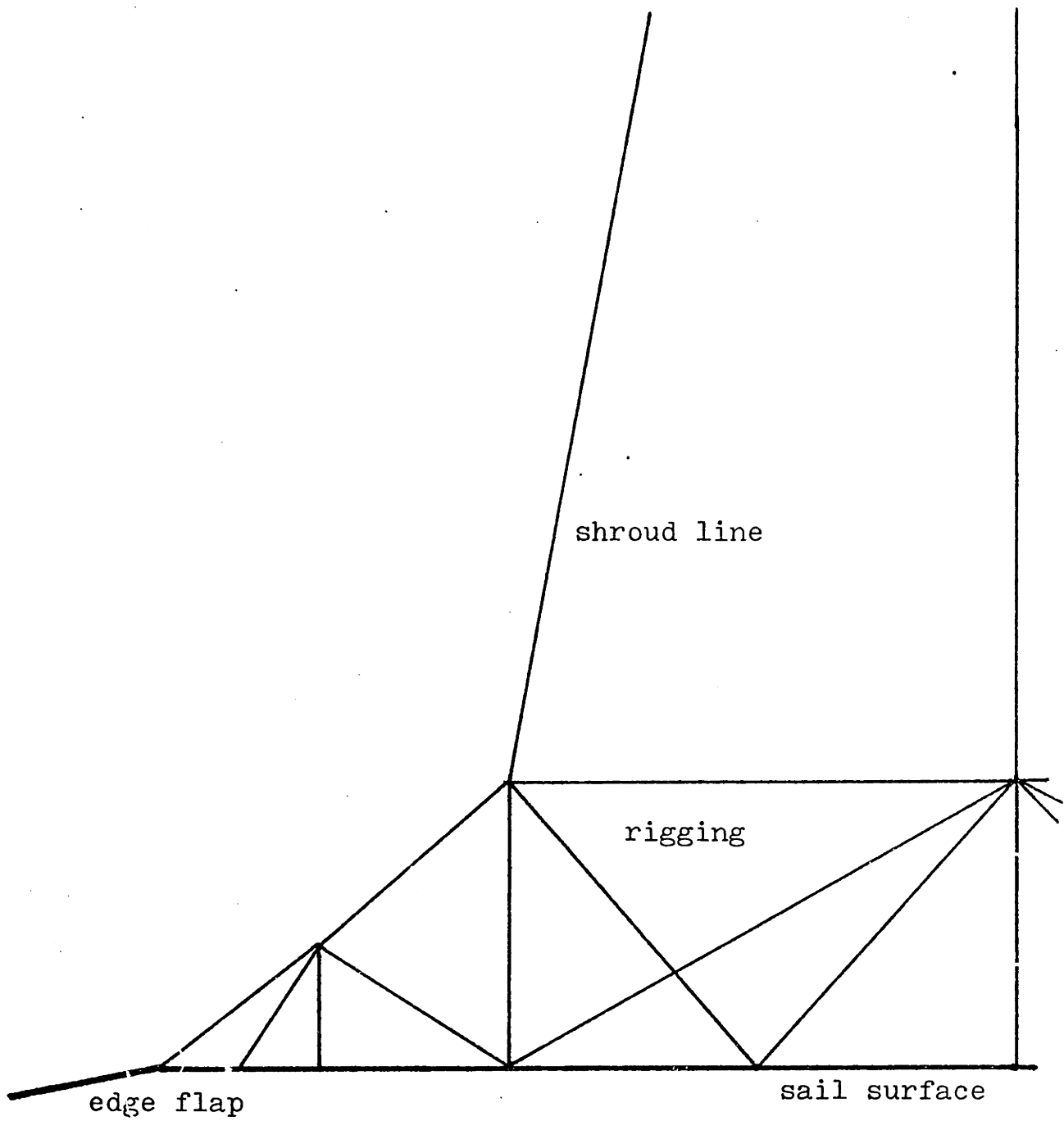
shroud line

rigging

edge flap

sail surface

Figure 3.8:   Half of rigging for a 2.4 km sail

payload

ballast mass

sail surface
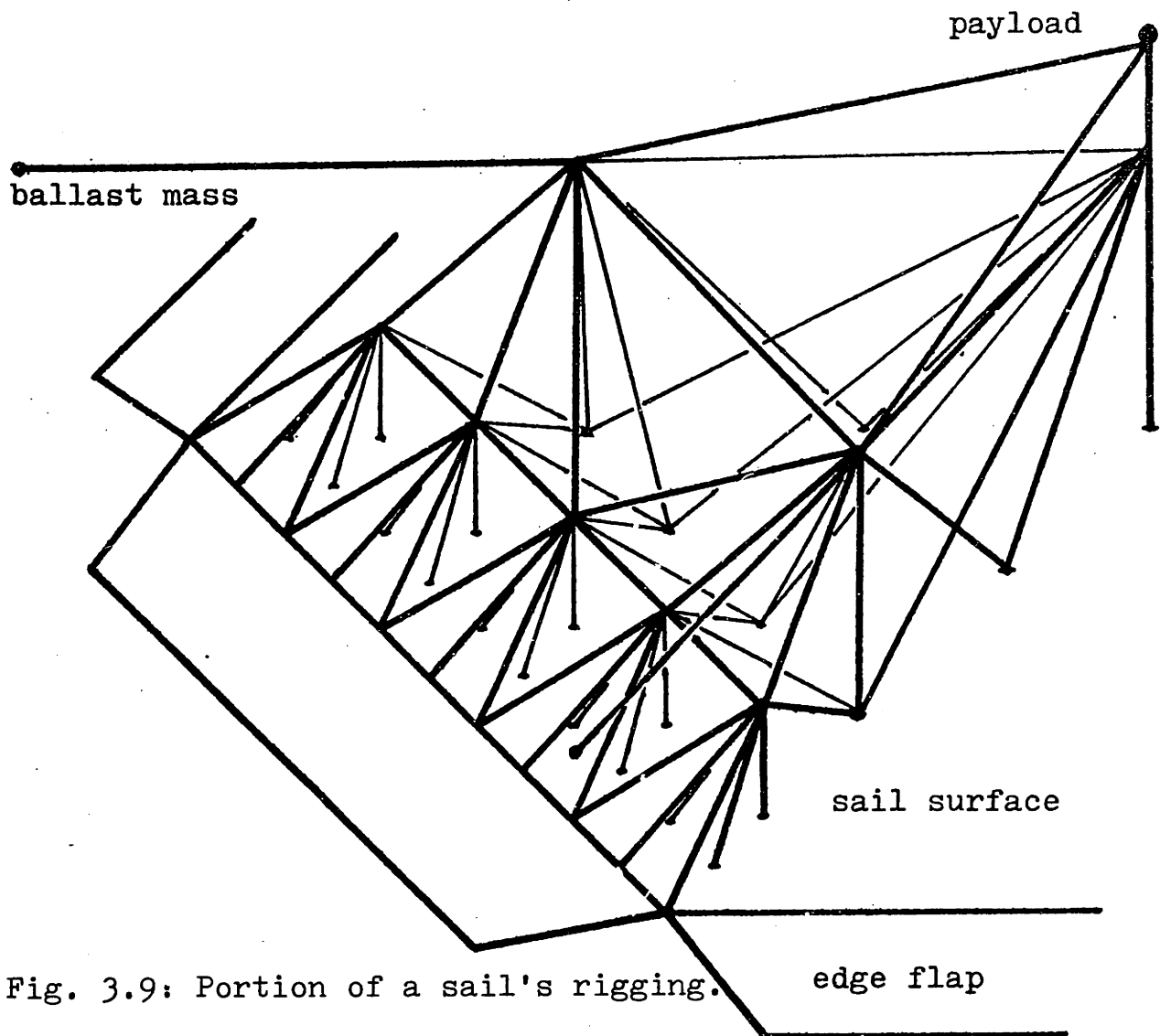
Fig. 3.9: Portion of a sail's rigging.　　edge flap

Under the maneuvering loads experienced in one of the sail control modes, stresses in the sail can be redistributed substantially. The rigging shown in Fig. 3.8 provides for this, although some of the redundant members from points high in the rigging may go slack.

In either mode, the rigging's primary job is to concentrate the force of light pressure from the bottom of the rigging and to transmit it to the top. Taking the thickness of the rigging as 0.4 times the radius of the sail, the rigging mass per unit area is approximately $0.4(RC_dE/s)$ gm/m^2, or 0.8E times

the mass of the structural grid in the sail sheet. Taking E=0.2 as before, the rigging adds about 16% to the structural mass of the sail. However, maneuver loads and minimum gauge considerations could be quite significant. Therefore, the balance of this study will assume a rigging mass 30% that of the grid.

3.5: The non-film mass of the sail

Independent of the mass of the film, the sail has components with a certain mass per unit area. This mass may be broken down into that of the foil springs (which link the reflecting sheets of the in the panels), the tension structure making up the rest of each panel, the main tension structure of the sail (grid plus rigging), odds and ends at the nodes in the structure, and controls, actuators, and payload interface structure. All mass densities below are in grams per square meter of the reflecting area of the sail.

Clusters of foil springs link the corners of six foil triangles together, each under a tension of about 0.0015 N. Each spring cluster might be made from six strips of steel foil (1 cm by 0.5 mm by 25 microns) mounted on a steel foil base (0.4 cm in diameter and 25 microns thick). These add a mass density of 0.00731 to the sail.

The JPL sponsored solar sail study selected a graphite-polyimide material for use in the primary tension structure of the Heliogyro sail. This material was presumably selected for its high strength-to-density and modulus-to-density ratios, as well as for suitability for roll deployment and space use. On the basis of this, the same material is proposed for the

primary tension structure in the present design. It has a strength in excess of 500 MPa, a modulus of 125 GPa, and a density of 1.52 gm/cm^3. It is available in strips with a thickness of 25 microns; thinner strips had a "gauzy" appearance and a lower modulus (JPLpcomm). Although the modulus is not critical in the present application, the 25 micron material will be assumed, even in minimum gauge members.

Micrometeoroid damage constrains minimum gauge tension member design to a degree that varies with the length, load, acceptable failure probability, and design life. This study will employ non-optimized "minimum gauge" tension members made from three parallel strips of graphite composite, each 25 microns thick and 0.25 mm wide. To enhance micrometeoroid damage tolerance, ring-shaped spacers (each 1 cm in diameter, 2 mm long, and 25 microns thick) separate the strips and redistribute loads if strips fail. Altogether, this member has a mass of 0.0333 gm/m. Its strength is over 9 N initially, falling to 3 N when two of the strips have failed. This is more than adequate, since contemplated loads are closer to one newton. The damage model described in MacNeal, 1968, gives a 0.001 chance of failure for a 100 meter length in 25 years of micrometeoroid exposure. Framing the panels with catenary cables of this design adds a mass density of 0.00286 to the sail.

Links must be provided between this catenary cable and the corners of the film triangles at the edges of the reflecting panel. Since loads are extremely low, and a higher probability of failure (say, 0.01 per 25 years) seems acceptable, 3.9 mm wide strips of one micron thick titanium foil are proposed. Foil of this thickness has roughly one thousand times the strength needed, and may be made by vapor deposition (Pickhardt, 1977).

With a mass of 0.0176 gm/m and a total length per panel of about 310 m, these links add a mass density of 0.00136 to the sail.

Neglecting mimimum gauge limitations, the density of the main tension structure is proportional to the radius of the sail. Taking the mass given by the equation in Sec. 3.3 and the properties of the graphite-polyimide composite given above, stressing for operation at 0.5 AU, correcting for the fill factor of the sail, adding 30% for the rigging, and multiplying by a factor of 5 for safety, the main structure adds a mass density of only 0.00824 to a 10 km sail. This figure will be used below for smaller sails, adding a substantial element of conservatism.

At the nodes in the main tension structure will be empty reels left over from the structure's deployment, some springs and possibly dampers, and a bit of connecting structure. As will be seen in Chapter 4, the reels are small, about 4 cm in radius. The springs and dampers carry modest loads (tens of newtons) over modest distances (fractions of a meter, to achieve load redistribution). Each node will be assumed to have a mass of 20 gm, adding a mass density of 0.00247 to the sail.

The shroud lines carry the light pressure loads from the top of the rigging to the payload. If the payload is 1.5 sail diameters above a 10 km sail, and if the graphite composite is used again, the shrouds add a mass density of 0.00610 to the sail. Again, use of this figure for smaller sails is conservative.

This completes the listing of the non-film elements of the sail, save only the control systems, actuators, and payload interface structure. These will be accounted for by adding 10% to the total non-film mass of the

sail. Table 3.1 summarizes these results: Including the 10% allowance, the non-film mass for a 10 km sail amounts to roughly 0.03 gm/m^2.

The above is essentially a point design; many parameters could be traded off against each other, and the elements could be subjected to more careful design and mass estimation. However, since this estimate suggests that the non-film mass makes up less than half the mass of a sail incorporating 15 nm films, and only 10% of the mass of one incorporating 100 nm films, its exact value is less than crucial to sail performance estimates. The greatest uncertainties by far arise from the thin films themselves.

Chapter 4: Sail Construction

4.1: Strategy

The strategy for near-term sail construction is to make and assemble as much of the sail as possible on Earth. Thus, while the delicate films must be made in space, all other components are made on Earth. While the panels (being made from these films) must be assembled in space, the balance of the structure is deployable. The advantage of such an approach is obvious.

The sail construction system consists of the following elements: a scaffolding (to control the structure's deployment), the film fabrication device (already described), a panel assembly device, and a "crane" (slung on tension members attached to the scaffolding) for conveying panels to their installation sites. The balance of this chapter will present conceptual designs for these system elements, descibe their operation, and make rough estimates of their masses.

4.2: The scaffolding

Since the sail is to be a rotating, centrifugally tensioned structure, there are strong arguments for making the scaffolding similar. However, while the sail may be tensioned in the axial direction by light pressure and payload inertial reaction, the scaffolding must incorporate axial compression members. If these members are to lie outside the sail and are to share its six-fold symmetry, a design somewhat like that shown in Figure 4.1 results.

This structure rotates at a rate within the operational envelope of the sail itself, to facilitate the sail's release. The six compression members define the vertical edges of a hexagonal prism. Many tension members parallel to the base link these compression members to support them against centrifugal loads. Ballast masses slung further from the axis provide additional radial tension and rigidity near the top of the scaffolding. Other tension members (not shown) triangulate the structure for added rigidity. Tension members span the base of the prism, supporting a node at its center. The interior is left open, providing a volume for deploying and assembling the sail. The top face is left open, providing an an opening for removing it.

Figure 4.2 illustrates how the deployed sail would be held in the scaffolding. The face of the sail is near the top of the scaffolding, and the rigging below. If the scaffolding is oriented properly, the sun will shine on the usual side of the sail, making it pull up on its attachment point at the base of the prism. The total thrust of the sail is then an upper bound on the axial load supported by the compression members. For a 2.4 km sail, this is less than 5 N per spar. 4.3: Scaffolding deployment
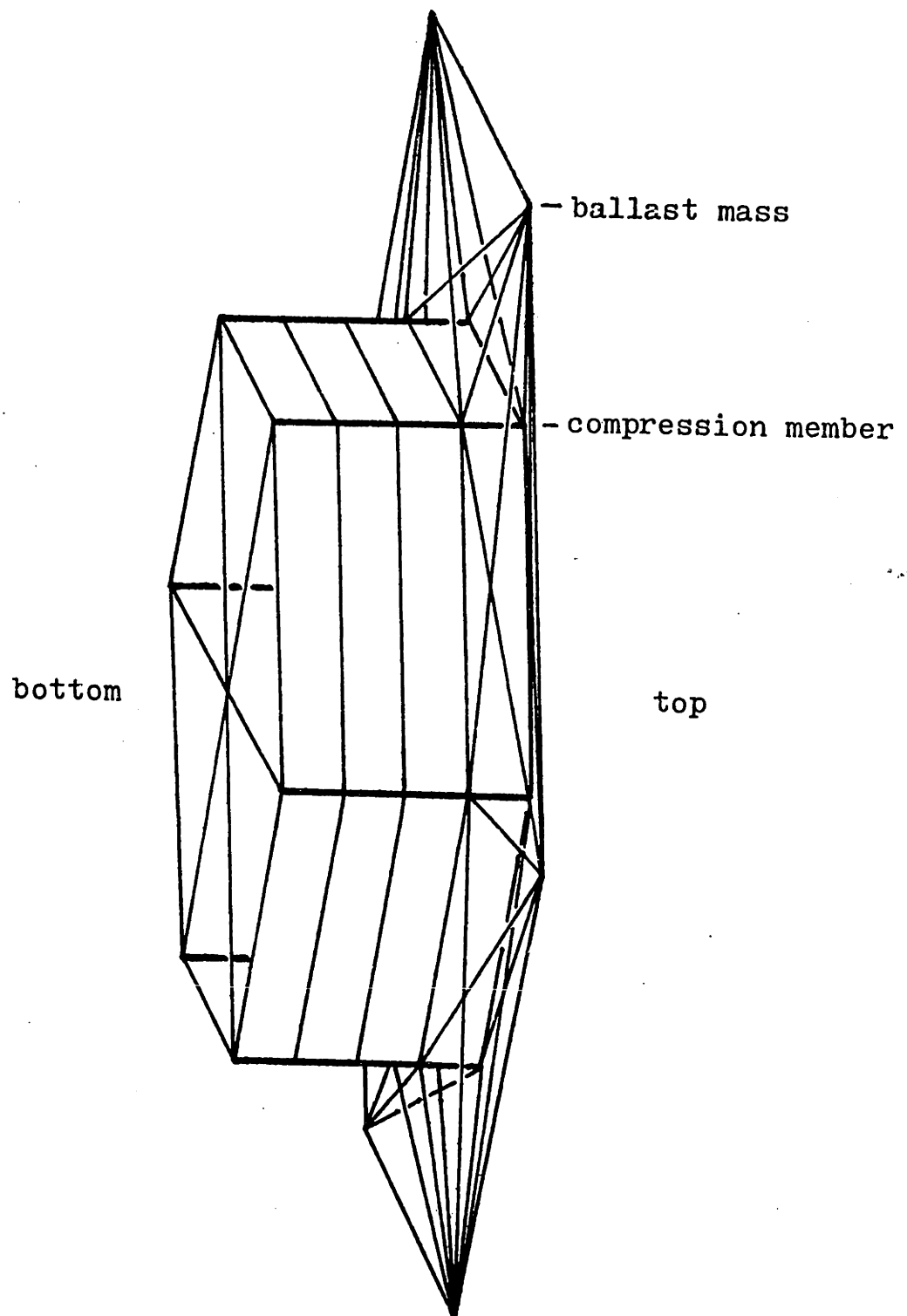
—ballast mass

—compression member

bottom

top

Fig. 4.1: Scaffolding for sail deployment and assembly. Hexagonal "box" encloses sail.
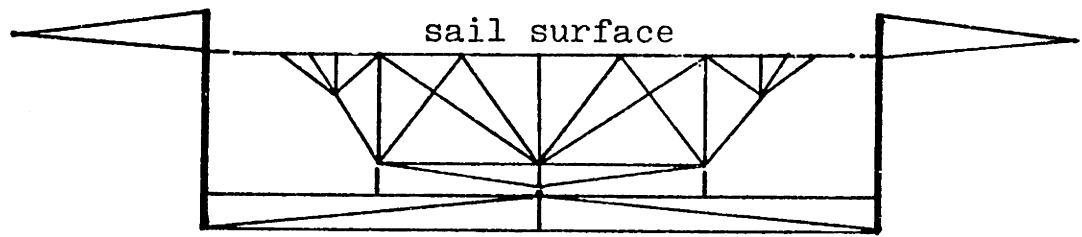
sail surface

Fig. 4.2: Deployed sail in scaffolding.
(compare to Fig. 3.8)

It is clearly desirable to make the scaffolding a deployable structure, if sails are to be a near-term project. Fortunately, JPL's work on a square, spar-supported, deployable solar sail design has helped lay the groundwork for such concepts. The JPL design was an astromast and stay structure, with the astromast spars carrying loads comparable to those contemplated here. Spar lengths are also comparable. While the scaffolding differs in being centrifugally tensioned and thus has loads perpendicular to the spars, the spars can be supported against these loads at short intervals by subdivided tension members. Thus, development times and costs should not be radically different.

Figure 4.3 illustrates one deployment-sequence concept. The six astromast spars, still in their cannisters, are first deployed from the center body to their operational radius by centrifugal force. This process is controlled by the pay-out rate of lines from the center body. At full radius, the spin rate would be a small fraction of the operational value, to reduce loads on the system as the spars deploy. After spar deployment,

ballast masses are lowered into their operational positions, and small

rocket motors on them spin up the structure to its operational rotation

1

2

3

comp.
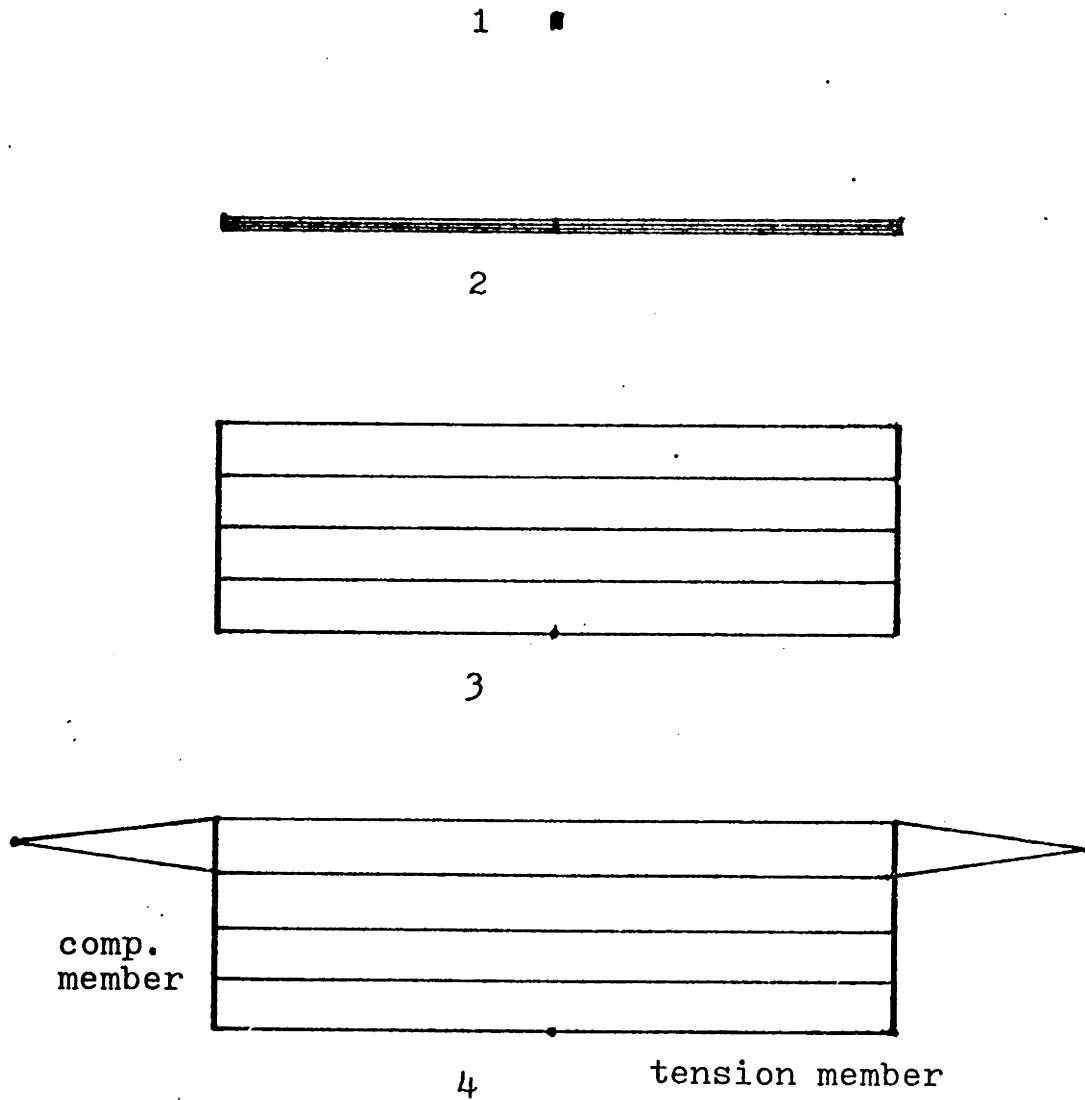member

4   tension member

Fig. 4.3: Scaffolding deployment, schematic.

rate.

4.4:   Sail structure packaging and deployment

The sail's structure consists of a regular grid of tension members, springs, and dampers, and a less regular three dimensional network of rigging. It would be a complex object to assemble in space. Fortunately, even the structure for a sail much larger then that discussed here can be tucked into the Shuttle payload bay in deployable form.

Since the sail is a pure tension structure, its structural elements can be wound up on reels. Conceptually, the grid structure can be shrunk into a regular array of reels in a plane, with each node in the grid represented by a housing containing three reels. The rigging can be shrunken into a less regular array, and the nodes containing its reels stacked on top of those of the grid.

If the tension members add 30 microns to the radius of the reel with each turn (a generous estimate), then the 115 m long elements will fit on reels with hub and external radii of 1.5 and 3,7 cm respectively. Springs and dampers could be stowed above or below the reels. Allowing 0.3 cm clearance between the edge of the reel and the edge of the housing, a 2.4 km sail structure fits into a 1.7 m wide package: small enough for table-top assembly.

The structure will be deployed by pulling on cords attached to certain nodes. Deployment may be controlled by friction brakes in the hubs of the reels. By setting the brakes properly, positive tension must be applied for deployment, and certain members may be made to deploy before others. Further control of the deployment sequence, if needed, may be introduced by

mechanisms which prevent some elements from beginning to deploy until selected adjacent elements have finished deploying. If detailed external intervention is deemed desirable, brakes could be rigged to release when a wire on the housing is severed by a laser pulse. Laser systems capable of this (even for less cooperative targets) should be readily available in the early 1980's.

The major concern in deployment of the sail structure is avoidance of tangles. Making the reel housings of a rounded shape will help. A deployment sequence in which the members are kept taut, and the complex rigging is spread out and gotten out of the way early in the process seems desirable. The bag of tricks outlined above should suffice to make the elements deploy in the desired sequence, but such control might not prove necessary. A subscale test of deployment could be a valuable Shuttle experiment.

4.5: Panel assembly

A film fabrication device and a panel assembly device together form a panel fabrication module. Figure 4.4 illustrates a conceptual layout for such a module, which would assemble two panels at a time from the output of one film fabrication device.

The film fabrication device produces a steady stream of film triangles mounted to foil spring clusters at their corners. The panel fabrication device takes segments of this stream (perhaps incurring a loss of 1% or so by discarding sheets between segments) and conveys them along a track to assembly stations. There, each segment is fastened to the previous segment
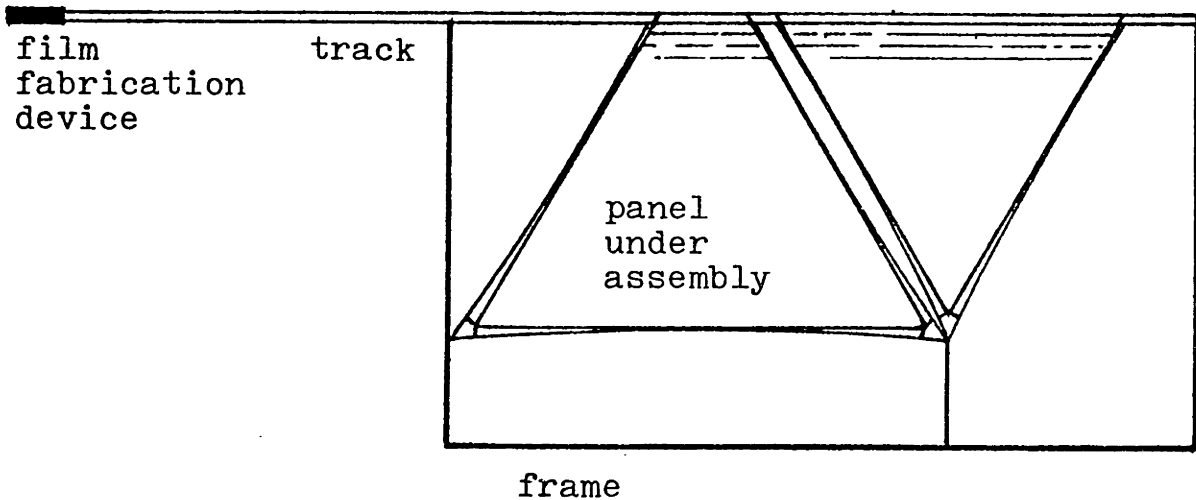
Fig. 4.4: Panel fabrication module layout.

and to the edge tension members that will frame the finished panel. This non-steady process of panel assembly requires a length of track to serve as a buffer with the steady film production process. Since interruptions need be no more than a few seconds, a few tens of meters of buffer track should serve.

At the assembly stations, the segments are transferred to fixtures with a lateral transport capability (Fig. 4.5). During transfer, each segment is bonded to the one before along one edge. While the next segment is brought into position, the last segment (now a part of the panel) is indexed over by one strip width, completing the cycle. Special devices bearing edge tension members travel on tracks and place foil tabs from

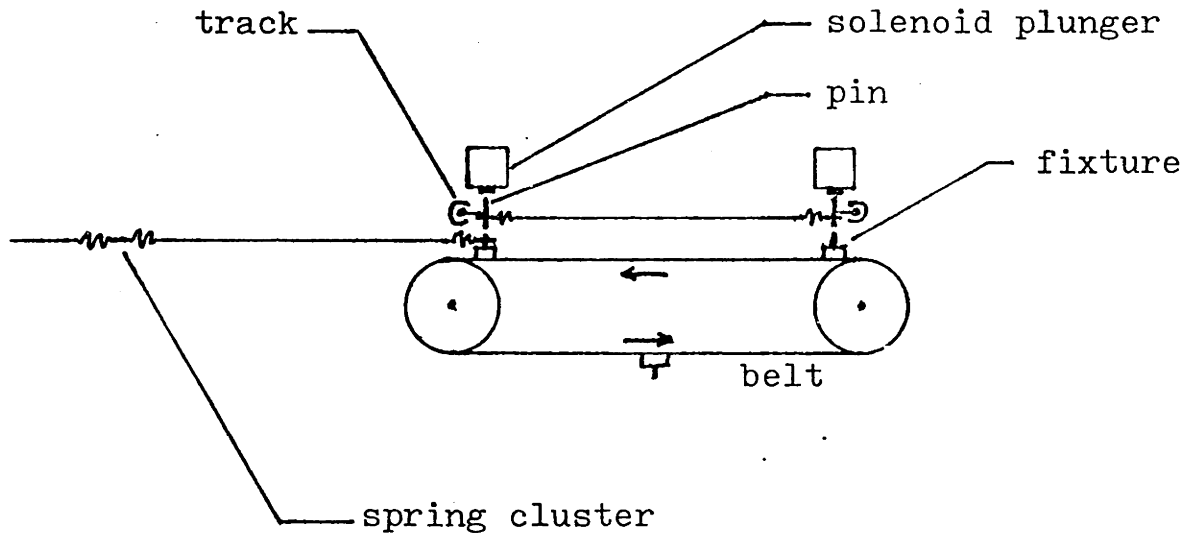these members in position for bonding by the same mechanism, to complete

Fig. 4.5: Schematic of assembly station in panel fabrication device.

the panel structure.

The foil tabs linking the segments may be bonded to one another in many ways, including ultrasonic welding, spot welding, and stapling. Attachment and conveyance may be integrated if the foil tabs are hooked over pins for conveyance. These same pins can be the tips of solenoid-activated tools that would cut and crimp two tabs together in a single stabbing motion. Similar pins and solenoids on the other side of the strip could perform the simpler transfer operation as well.

The panel assembly cycle ends with a pause, as the completed panels, now held only by their corners, are lowered into a storage region, and new

edge members are loaded into position. Further detail in the panel assembly concept will be passed over for the sake of brevity.

4.6: Assembly of panels to the sail structure

At this point, the sail's structure is deployed within a scaffolding, and panels are being produced and stored at a panel fabrication module. The need, then, is for a system that will accept stacks of stored panels, convey them to apertures in the sail's grid, and install them.

The stored panels are initially located at a node suspended on tension members above the center of the sail. A crane is likewise suspended, but from tension members terminated in actively controlled reels mounted on devices free to move around the top of the scaffolding. This makes it possible to position the crane over any aperture in the grid. Bridles give it freedom to turn (to match the orientation of the aperture); other bridles allow it to move up and down.

All of these motions require but one type of element: a device which can, on command, change its position along one tension member while reeling or unreeling another. Operational sequences may readily be devised which permit these devices to run on local solar cell panels of modest size (one square meter or less), sidestepping possible power distribution problems. Command signals would be broadcast by a central controller. Since these devices are the main variety of active element in the sail assembly process, making them reliable and combining them in redundant ways will go a long way towards making the sail assembly system reliable. The motions involved in panel installation can be rather slow; an installation rate of

around one per hour keeps up with the panel production rate.

The crane is loaded while docked to the panel storage frame, and panels are installed while it is docked to the appropriate aperture in the structural grid. Docking in both cases is effected either by mechanical arms or by a compliant mechanical system. Loading might best be accomplished in a hard docked mode for transfer of several panels on a conveyor. Installation is accomplished by removing a panel and hooking its corners onto nodes in the grid. This should not require very precise positioning of the crane.

4.7: Sail release

Once panel installation is complete, and the operation of various reels has been checked, the sail is ready for release and use. It is already spinning at a rate within its operational envelope, and is already under thrust, hence this task may not be difficult. The proposed method is as follows.

First, the sail's path must be cleared. To do this, the film fabrication device, its power supply, the panel assembly device, and the crane are conveyed to the sides of the scaffolding in a balanced fashion (maintaining the center of gravity within bounds is an issue in this process). The top face is then clear of objects and tension members. Then, the members holding the corners of the sail are released, and the remaining restraint points brought forward to carry the sail half out of the scaffolding. Finally, all restraints are released, and the sail rises free.

Chapter 5: Solar Sail Dynamics and Control

Passing over the translational motion of the sail as a whole, sail dynamics may be divided into rigid-body motion and internal vibrations. Regarding rigid-body motion, the aim is to show how the sail's attitude can be stabilized and changed on command. This will be discussed in the context of the two control modes mentioned above. Regarding vibrations, the aim is to show how the sail can avoid damage from vibrational loading.

5.1: Mode 1 dynamics and control

The mode 1 sail configuration is illustrated in Fig. 5.1. In this mode, for any value of the payload mass, the symmetry axis is the axis of maximum moment of inertia. Therefore, rotation about this axis is stable. In this mode, control forces are small, and perturb the stress distribution in the sail only slightly. Therefore, the considerations discussed in Sec. 3.2 hold, and show that the sail may be treated as a rigid body.

In mode 1, tilting of panels produces control forces. The panels may be tilted as shown in Fig. 5.2: small electric motors reel or unreel lines on command, so as to move the panel corner up or down while maintaining
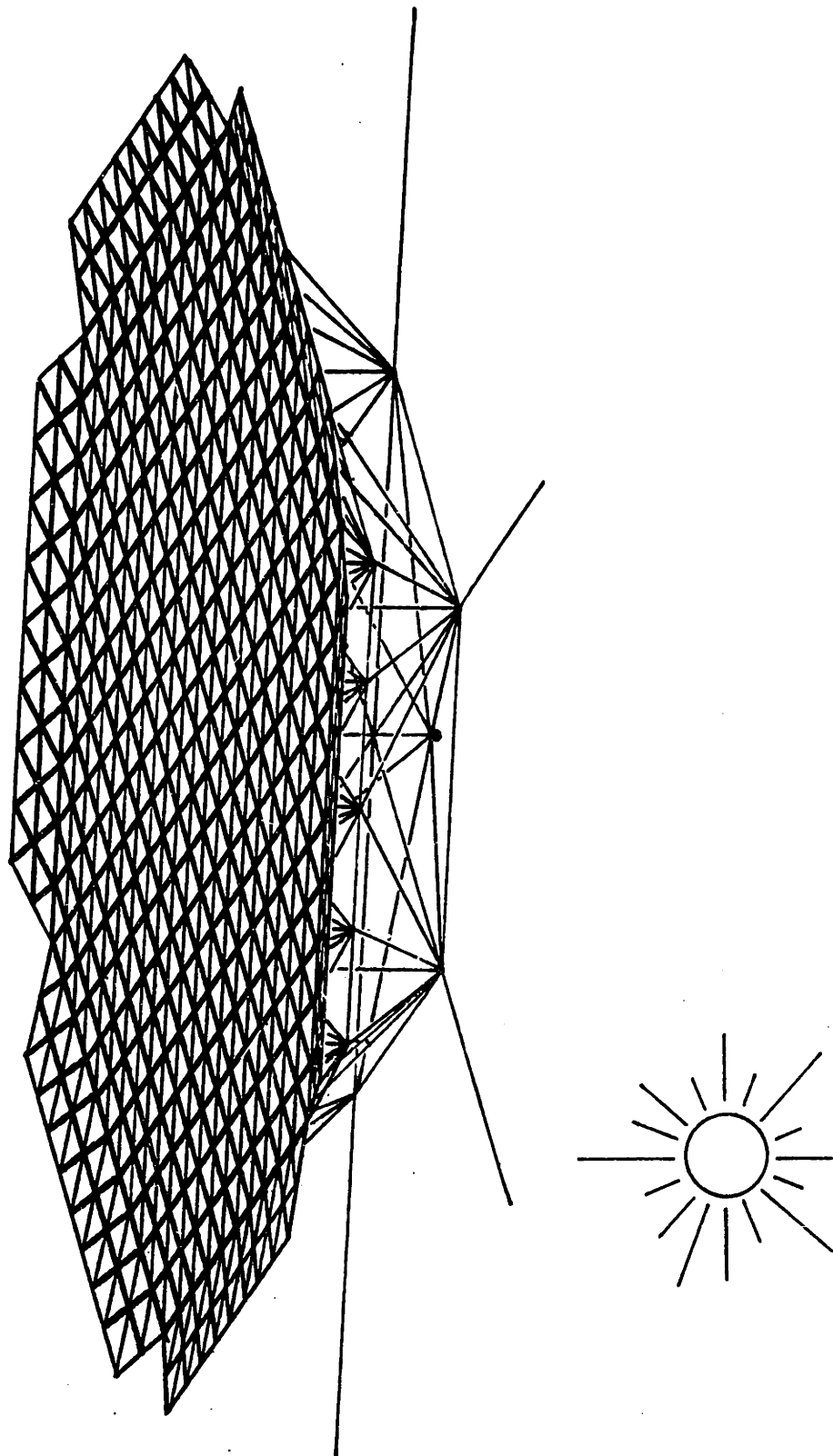
Fig. 5.1: Mode 1 sail configuration

proper tension on it. Each panel has a mass of some 0.3 to 1.1 kg. Since the control units can probably be made in the fractional kilogram range (they need only milliwatts of power), they will not add much to the mass of the sail so long as only a small fraction of the panels need be tilted. This mode may be made highly reliable by providing redundant tiltable panels. 5.1.1: Attitude stability

Since mode 1 is conceived of as a semi-passive control mode for interplanetary cruising (where only slow changes of attitude are needed), it is of importance to consider the stability of a passive sail set at various angles G to the sun. Figure 5.3 illustrates the sail/sun geometry, with the x-axis pointing away from the sun, the y-axis (at an angle G to the x-axis) pointing along the axis of the sail, and the z-axis perpendicular to the others. By symmetry, no torques should act along x or y. In the ideal sail approximation (planar, perfectly reflecting), thrust will be normal to the sail and act through its center of area, that is, along the axis of symmetry. Hence the ideal sail experiences no torque in any position, and is neutrally stable: an encouraging result.

Now consider an absorbing sail. Its thrust may be divided into purely reflective and purely absorptive components. The first produces no torque (as above), while the latter produces a torque about the z-axis proportional to $\sin(G)\cos(G)$. To counter this torque, light pressure must be increased on the far side of the sail from the sun relative to that on the near side. Making the sail concave towards the payload does this.
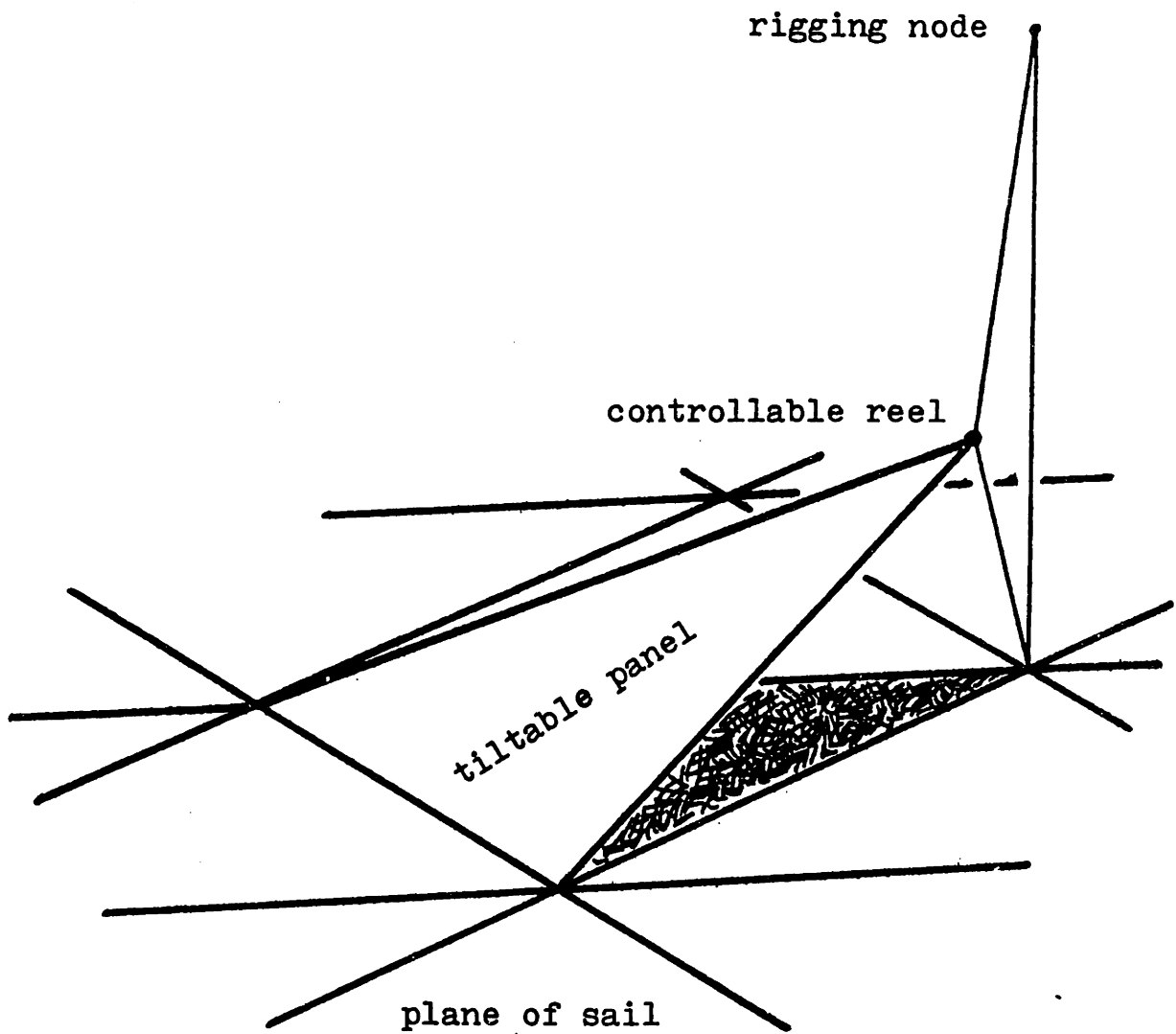
rigging node

controllable reel

tiltable panel

plane of sail

Fig. 5.2: Panel tilted for sail control.

x-axis

G

y-axis

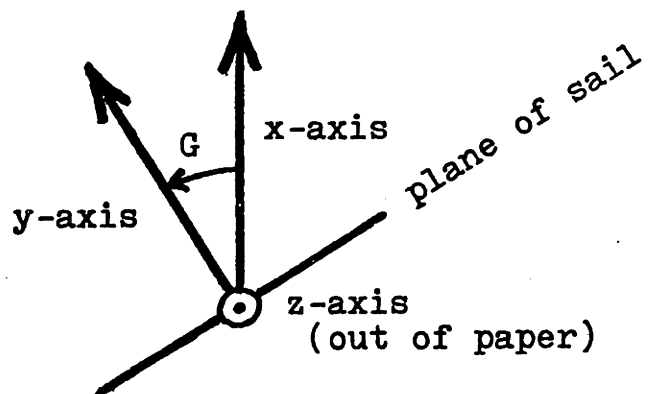plane of sail

z-axis
(out of paper)

Fig. 5.3: Sail coordinate system

For a given sail surface shape, assumed nearly flat, this balancing torque will be very nearly proportional to the first derivitive of the normal sail thrust with respect to G. Since both the absorptive and reflective components of the normal force are proportional to $\cos^2(G)$, the derivative is proportional to $\sin(G)\cos(G)$. Thus, the perturbing torque and the correcting torque vary together, and a constant sail concavity yields neutral stability in this rather good approximation. The required concavity for a typical sail is several degrees.

The only other sail non-ideality of any consequence is due to light scattering from undulations in the sail surface. For modest values of G, this small effect closely resembles an additional absorptive component of thrust. At higher values of G, it falls off more quickly than the absorptive component. Hence, it may be compensated for quite well at most sail angles of interest by increasing the sail's concavity slightly. Complete correction can be effected at any sail angle by setting the angle of a few trim panels.

5.1.2: Attitude and spin rate control

Since torques can be balanced at all sail angles of interest, small perturbing torques can shift the sail from one attitude to another, or

change its rotation rate. Rough calculations are in order to give some indication of the number of tiltable panels needed for interplanetary cruise missions.

Since heliocentric orbit times are typically months, spin-up and spin-down times of 10 days and precession rates of 0.1 radian/day seem reasonable targets. Tilting a panel by about 20° changes the force on it---both normal to the sail surface and parallel to it---by about 30% of the panel's maximum thrust. Allowing for various geometric factors in panel orientation and efficiency of thrust application for various tasks, perhaps 10% of the maximum thrust (on the average) is actually useful for a given maneuver.

Both of these target capabilities require the same time rate of change of angular momentum. For both, the worst case is that of a large, low-performance sail. For both, simple calculations show that the target capability can be met, even for a 10 km diameter sail of the lowest probable performance, by tilting fewer than one panel in a hundred. The smaller sail structure shown in Fig. 5.1 provides locations suitable for 106 tiltable panels out of a total of 828.

Simply tilting the panels so as to increase or decrease the average concavity of the sail effects precession about the x-axis. Tilting selected panels up and down as the sail rotates can produce a gradient in the average normal force on the sail in the z direction, effecting precession about the z-axis and thereby changing G. Maximum panel corner speeds required for this are a fraction of a meter per second. Tilting panels in a pinwheel pattern changes the spin rate about the y-axis. Finally, active control of panel tilt can damp nutation, if energy

dissipation in the structure does not suffice.

Tilting panels to effect changes in the spin rate may produce torques tending to change G as well. These torques may be compensated for by active control like that intended to change G alone.

Thus, sail operation in the mode 1 configuration is characterized by torques that may be balanced by a few statically positioned trim panels, permitting an entirely passive cruise mode. Slow changes in the sail's attitude and spin rate may be made, from time to time, by cyclic variation of panel tilt to produce perturbing torques. The passivity of cruise mode and the ease of providing redundant tiltable panels recommends this mode for reliable interplanetary transportation.

5.2: Mode 2 dynamics and control

In the mode 2 sail configuration, the payload mass will be assumed to be large compared to the sail mass, and the sail will be considered as a separate object linked to it by actively controlled shroud lines. So long as the forces exerted by the shroud lines keep the rigging taut, the considerations discussed in Sec. 3.2 hold, and the sail may be treated as a rigid body.

In mode 2 (as in mode 1), tilting of panels controls the spin rate. However, in this mode precession is effected by varying the tension exerted by the shrouds on different parts of the sail. This is accomplished by reeling and unreeling the shrouds in a coordinated fashion as the sail turns. Maximum reel speeds in small sails are a few meters per second.

Kinematically, a precessing disk experiences a uniform gradient of

normal acceleration across its surface. For a sail anchored to a massive payload, the average acceleration over the surface of the sail will be near zero. Limiting the maximum normal acceleration to the characteristic acceleration of the sail Ac (m/s^2), the maximum rate of precession P (rad/s) will be Ac/v, where v is the rotational velocity at the rim of the sail. Incorporating previously made assumptions about the sail's rotation rate leads to P=(Ac/RE)$^{0.5}$, where R is the radius of the sail in meters.

For the 2.4 km sail discussed above, and the probable range of sail performances, this implies precession rates of 13 to 26 rad/100 minutes, when the sail is flat on to the sun. This provides a generous margin in turn rate, even for maneuvers in low Earth orbits. Substantially larger sails or substantially smaller acceleration gradients across the disk would still allow adequate turn rates for this important application (turn rates around 3 rad/100 minutes suffice for polar escape spirals).

As in mode 1, active control permits damping of nutation. This is important, since nutation would otherwise be initiated by rapid changes in precession rate. It should be noted that during precession the payload is offset from the axis of rotation in a direction fixed in inertial space. Characteristic times for changes in payload offset can be quite short.

5.3: Mode 1/Mode 2 interconversion

For missions involving both interplanetary cruise and circumplanetary maneuvering, a vehicle able to operate in both modes is desirable. Mode 1 has a decisive advantage near planets (because of its maneuverability), but cannot enter a passive cruise mode. The greater distance between the

payload and the sail in this mode precludes balancing the torque on the sail resulting from absorbed light with a reasonable amount of concavity, as is done in mode 1. Instead, this torque must be countered in the same manner as the sail is precessed: by active manipulation of shroud tension. While control of shroud tension might be made redundant by placing reels at both ends of the lines, reliability still favors a passive system on long missions. Fortunately, interconversion seems simple. Mode 2 control can be maintained as the shroud lines are reeled in, so long as the sail is properly ballasted for mode 1. When the payload reaches the mode 1 position, the reels can be locked and mode 1 control begun.

5.4: Vibrations

The major sources of oscillating loads in the sail are control forces, thermal cycling, and (in some orbits) gravity gradient forces. All of these have periods equal to the rotation period, some have components at higher frequencies. Control forces are small in mode 1 and substantial in mode 2. Thermal cycling produces distortions of about (deltalength) m in kilometer long members. Gravity gradient forces are small.

Since the sail structure is a truss, damping from the structural materials alone may be adequate. Since deformation can be concentrated in spring/damper combinations at the nodes, strong damping can be introduced very efficiently. So long as resonant excitation is avoided, structural vibration should not reach harmful levels. Since the major sources of excitation act at the sail's rotational frequency, modes with frequencies at least five times this frequency should experience little excitation.

Even in the absence of rigging, the sail sheet's lowest mode (in out-of-plane vibration) would have a frequency about 2.3 times the rotation rate (Lamb, 1921). Rigging brings bending stiffness into play, since its members must be stretched and compressed as the sheet deforms. It is easy to show that a stiffness as small as a few tens of newtons per meter of elongation in the upper rigging members raises the frequency of the lowest mode to over five times the rotation rate, for the 2.4 km sail. Far larger sails should present no problems in this regard.

Stretch modes in the sheet have still higher frequencies, as do the plucked-string modes of taut tension members and panels. The edge flaps have pendulum-frequencies only 2.5 times the rotation frequency, but if necessary they may be stiffened with additional tension members.

Slack tension members have low vibration frequencies, but show non-linear response. As vibrations build up to significant energies, the members become taut, raising their frequencies. Frequencies exceed five times the rotation rate long before a risk of damage appears.

In short, the body of the sail can be made comparatively stiff, and can be damped very well. It promises to be a well-behaved structure.

In mode 2, however, the dynamics of the shroud lines presents a more complex problem. They are long, and maximal precession rates require varying the tensions on them, at the sail's rotational frequency, with maximal variation of tension. With proper rigging design (resembling that of the mode 1 or convertible sail), the shroud lines may be drastically shortened with little sacrifice in turn rate, and even less in acceleration. The shroud lines are another candidate for the addition of

stiffening tension members to raise vibrational frequencys.

Thus, the shroud lines are simply another part of the body of the sail in mode 1, and mode 2 can be made very similar to mode 1 with little sacrifice. Further, long shrouds (with lighter, ballast-free rigging) may be well-behaved, particularly since tension on them can be actively controlled. Finally, the shrouds can be linked to reduce their free, undamped lengths. Hence the balance of the sail's tension structure promises to be a well-behaved structure, one way or another.

Concern might arise that uncertainties in the feasible film areal mass density might hold up design of the structure. If the parameter E (or its range of variation) is kept a design condition, to be maintained by choice of spin rate, then loads on the structural members will be a constant, independent of the areal mass density of the sail sheet. Further, the various pendulum frequencies of the elements, and of various modal frequencies of the sail remain in a constant ratio to the spin rate as the mass density varies. Thus a sail may be designed with comparatively little regard for the film mass density or any · remaining uncertainties in it.

Conclusions:

The properties of thin aluminum films have been reviewed. Layers 15 nm thick approach bulk reflectivity. Layers 100 nm thick have shown strengths many hundreds of times that needed in the sail application. Calculated equilibrium temperatures at 0.5 AU appear survivable. The possibility of reinforcing aluminum films with films of other materials was examined and found to be of interest. A concept for imparting tear resistance to thin films by means of controlled patterns of stress relief

was outlined and found attractive. Although further work is needed on film element design, film properties appear to have little impact on the balance of the sail system. Experimental and analytic work is needed on film properties, element design, and interactions with the space environment.

Various candidate methods of film element fabrication were reviewed, and a process based on use of a subliming parting layer was selected. A device embodying this process was discussed in some detail, including preliminary mass estimates. The author produced sample aluminum films using a soluble parting layer process and verified their ability to survive handling and stresses believed to be representative of the proposed fabrication process.

Structural concepts proposed for deployable sails were reviewed. To take full advantage of the performance potential of thin film reflectors, a centrifugally-tensioned disk, made rigid by a pure-tension truss structure, was derived. A concept involving incorporation of film elements into modular panels was proposed. An estimate of the total non-film mass in the sail, including the panel structure, the main structure, control actuators, and structure deployment hardware amounted to some 0.03 gm/m^2, for a sail of 10 km diameter.

A concept for sail construction was outlined, involving a deployable main structure, and a deployable scaffolding. The scaffolding employs astromast compression members comparable to those proposed for one of the JPL solar sail designs for its axial structure. It is tensioned in the radial direction by rotation at a rate compatible with sail release. Devices for panel assembly and installation were also outlined.

Control of the sail's attitude with respect to the sun was considered.

Two control modes were derived, one based on panel tilt to produce precessing torques, and the other based on payload offset. The former is slow, but involves no failure critical moving parts and permits an entirely passive cruise mode. It appears desirable for interplanetary flight. The latter is swift enough to permit near-Earth maneuvering, but requires constant manipulation of shroud line tension. It appears that sails may be designed for conversion between the two modes.

In summary, a high performance solar sail system has been designed and subjected to preliminary analysis. While many questions remain, no barrier has been found to the production and use of solar sails with accelerations 20 to 80 times that of previously proposed, deployable sails. This higher thrust to mass ratio opens a wide range of missions to consideration, including orbit to orbit transfer in near-Earth space. Reduced mass is also expected to result in reduced cost per unit of thrust, opening the possibility that high performance solar sails will prove competitive for a variety of missions. Further examination seems warranted.

References:

Abeles, F. "Optical properties of metallic films." Physics of Thin Films, vol 6, p151 M.H. Francombe and R.W. Hoffman, eds., Academic Press, New York (1971).

Barnes, R.B., and M. Czerny, "Concerning the reflection power of metals in thin layers for the infrared." Physical Review 38:338 (1931).

Beecher, N., F. Feakes, and L.R. Allan, "Laminar film reinforcements for structural applications." Advanced Structural Composites, SAMPE National Symposium Exhibition, 12th, Western Period Co. North Hollywood, CA (1967).

Bennet, H. (ed.), Commercial Waxes, 2nd edition, Chemical Publishing Co., Inc., New York (1956).

Boiko, B.T., A.T. Pugachev, and V.M. Bratsychin, "Method for the determination of the thermophysical properties of evaporated thin films." Thin Solid Films 17:157 (1973).

Drexler, K.E., and H.K. Henson, "Design of equipment for vapor phase processing of metals," Lunar Utilization, D. Criswell, ed., Lunar Science Institute (1976).

Ferraglio, P.L. and C. D'Antonio, "Structure of vapor deposited aluminum films." Thin Solid Films 1:499 (1967/68).

Friedman, L., et. al. "Solar sailing---the concept made realistic." AIAA Paper 78-82, 16th Aerospace Sciences Meeting, Huntsville, Alabama, Jan 16-18 (1978).

Fritz, G. et.al., "Physical properties of diphenyl, o-, m- and p-terphenyl and their mixtures." Atomkernenergie 13:25 (1968).

Hall, C.E., Introduction to Electron Microscopy, 2nd edition, McGraw Hill, New York (1966).

Hass, G., and J.E.Waylonis, "Optical constants and reflectance and transmittance of evaporated aluminum in the visible and ultraviolet." Journal of the Optical Society of America 51:719 (1961).

Hemenway, C.L., D.S. Hallgren, and C.D.Tackett, "Near-Earth cosmic dust fluxes determined from Skylab experiments." Space Research XV, p.541 Akademie-Verlag, Berlin (1975).

Hoffman, R.W. "The mechanical properties of thin condensed films." Physics of Thin Films, vol. 3, p.211, G. Hass and R.E. Thun, eds., Academic Press, New York (1966).

Hunter, W.R. "The preparation and use of unbacked metal films as filters in

the extreme ultraviolet." Physics of Thin Films, vol 7, p43, G. Hass, ed. Academic Press, New York (1973).

JPL Working Paper on solar sailing, July, 1976.

Kirk-Othmer Encyclopedia of Chemical Technology, Vol 2, "Anthraquinone." p700, John Wiley and Sons, New York (1978)

Lamb, H. and R.V. Southwell, "Vibrations of a spinning disk." Proceedings of the Royal Society 99:272 (1921).

MacNeal, R. "Meteoroid damage to filimentary structures." NASA CR-869 (1968).

Maissel, L.I. and R. Glang, eds., Thin Film Handbook, McGraw Hill, New York (1966)

Milillo, F.F., C. D'Antonio, and R.W. Bauer, "Strength versus thickness in vapor deposited aluminum films." Thin Solid Films 3:51 (1969).

Pickhardt, V.Y., and D.L. Smith, "Fabrication of high-strength unsupported metal membranes." Journal of Vacuum Science and Technology 14(3):823 (1977).

Rustgi, O.P., Journal of the Optical Society of America 55:630 (1965).

Seraphin, B.O., "Chemical vapor deposition of thin semiconductor films." Thin Solid Films 39:87 (1976).

Smith, H.R., Jr., K. Kennedy, and F.S. Boericke, "Metallurgical characteristics of titanium-alloy foil prepared by electron-beam evaporation." Journal of Vacuum Science and Technology 7(6):S48 (1970).

Tsu, T.C., "Interplanetary travel by solar sail." ARS Journal 29:422 (1959).

Wiley, C., (pseudonym: Saunders, R.), "Clipper ships of space." Astounding Science Fiction, p135 (May, 1951).